Abcg2 labels multiple cell types in skeletal muscle and participates in muscle regeneration

Michelle J. Doyle,[1] Sheng Zhou,[2] Kathleen Kelly Tanaka,[1] Addolorata Pisconti,[1] Nicholas H. Farina,[1] Brian P. Sorrentino,[2] and Bradley B. Olwin[1]

[1]Department of Molecular, Cellular, and Developmental Biology, University of Colorado, Boulder, CO 80309
[2]Department of Hematology, St. Jude's Children's Research Hospital, Memphis, TN 38105

Skeletal muscle contains progenitor cells (satellite cells) that maintain and repair muscle. It also contains muscle side population (SP) cells, which express Abcg2 and may participate in muscle regeneration or may represent a source of satellite cell replenishment. In Abcg2-null mice, the SP fraction is lost in skeletal muscle, although the significance of this loss was previously unknown. We show that cells expressing Abcg2 increased upon injury and that muscle regeneration was impaired in Abcg2-null mice, resulting in fewer centrally nucleated myofibers, reduced myofiber size, and fewer satellite cells. Additionally, using genetic lineage tracing, we demonstrate that the progeny of Abcg2-expressing cells contributed to multiple cell types within the muscle interstitium, primarily endothelial cells. After injury, Abcg2 progeny made a minor contribution to regenerated myofibers. Furthermore, Abcg2-labeled cells increased significantly upon injury and appeared to traffic to muscle from peripheral blood. Together, these data suggest an important role for Abcg2 in positively regulating skeletal muscle regeneration.

Introduction

Skeletal muscle has a remarkable capacity to respond to pathological stress and regenerate upon injury. Skeletal muscle consists of postmitotic, multinucleated myofibers as well as mononuclear cells, including muscle progenitor cells (satellite cells) and other less well-characterized interstitial cells. Muscle regeneration is dependent on satellite cells, which in response to injury undergo proliferation, differentiation, and ultimately, fusion with new or existing myofibers to repair the muscle. Recently, the importance of other cell types located within the muscle interstitium has gained interest. Many of these, such as muscle side population (SP) cells, PW1+/Pax7− cells, vascular-associated pericytes, and myoendothelial cells have been reported to possess myogenic potential (Asakura et al., 2002; Dellavalle et al., 2007; Zheng et al., 2007; Tanaka et al., 2009 Mitchell et al., 2010). Others, including endothelial cells and fibroadipogenic progenitors (FAPs), positively regulate myogenesis (Abou-Khalil et al., 2010; Joe et al., 2010). In addition to these resident muscle cells, substantial evidence suggests regulatory interactions of the immune response with skeletal muscle play a significant role in regeneration (Tidball and Villalta, 2010).

Previous studies suggest that muscle SP cells may be precursors of the satellite cell population or may be independent progenitor cells that participate in muscle regeneration. The SP phenotype is defined by the ability of cells to efflux Hoechst 33342 dye. Abcg2, a member of the ATP-binding cassette (ABC) transporter family, effluxes Hoechst 33342 dye and is the molecular determinant of the SP phenotype (Zhou et al., 2001). Abcg2 also confers drug resistance in tumor cells by actively exporting multiple drugs and protects cells from apoptosis under cases of hypoxia and oxidative stress (Krishnamurthy et al., 2004; Krishnamurthy and Schuetz, 2006; Martin et al., 2008). Multiple tissues, including muscle, contain SP cells positive for Abcg2. In adult skeletal muscle, Abcg2-positive cells are closely localized to the vasculature (Meeson et al., 2004; Huls et al., 2009). Although previous studies show that muscle SP cells engraft into regenerating myofibers upon intramuscular transplantation (Asakura et al., 2002; Meeson et al., 2004; Tanaka et al., 2009), the fate of endogenous

Correspondence to Bradley B. Olwin: bradley.olwin@colorado.edu

Abbreviations used in this paper: ABC, ATP-binding cassette; eMyHC, embryonic MyHC; FAP, fibroadipogenic progenitor; FDG, fluorescein di-β-D-galactopyranoside; MyHC, myosin heavy chain; SP, side population; TA, tibialis anterior; VE, vascular endothelial.

The Rockefeller University Press $30.00
J. Cell Biol. Vol. 195 No. 1 147–163
www.jcb.org/cgi/doi/10.1083/jcb.201103159

muscle SP cells has not been traced in vivo, and so much about their identity and potential remains unknown. Upon genetic deletion of Abcg2, muscle SP cells are lost (Zhou et al., 2002), although the consequence of this loss on muscle regeneration has not been tested.

In the present study, we analyze the functional consequence of germline deletion of Abcg2 on muscle regeneration and show that muscle regeneration is delayed, resulting in fewer myonuclei and smaller caliber myofibers as well as a decrease in Pax7-positive satellite cells. Additionally, we followed the fate of Abcg2-positive cells in skeletal muscle in vivo using genetic lineage tracing driven by Abcg2 expression. Using this approach, we demonstrate that Abcg2-labeled cells contribute primarily to vascular-associated interstitial cells, including endothelial cells and pericytes. Upon injury, Abcg2-labeled progeny increases, although under these conditions, they are not a major contributor to myonuclei. We further show that the immune response is compromised in Abcg2$^{-/-}$ mice after injury. These data suggest that Abcg2 function in nonmyogenic cells affects signaling that positively regulates myogenesis.

Results

Expression of Abcg2 increases upon muscle injury

Expression of Abcg2 has been previously reported in progenitor cells isolated from skeletal muscle (Meeson et al., 2004; Tanaka et al., 2009). To determine whether Abcg2 expression is dynamically regulated during muscle regeneration, we isolated mononuclear cells from the tibialis anterior (TA) muscle of mice injured with 1.2% $BaCl_2$ at 2, 5, 12, and 30 d after injury as well as from uninjured TA muscles and analyzed the cells via flow cytometry for Abcg2 expression. We observed that in resting muscle, ∼22% of mononuclear cells express Abcg2 (Fig. 1, A and F). The mean percentage of muscle cells expressing Abcg2 increases significantly between 2 and 5 d after injury from 20 to 39% of isolated cells (Fig. 1, B, C, and F). At 12 d after injury, the percentage of cells expressing Abcg2 begins to decline, reaching levels similar to those of uninjured tissue by 30 d after injury (Fig. 1, D–F). The increase in Abcg2-expressing cells at 5 d after injury is consistent with the reported increase seen in tissue sections after cardiotoxin-induced injury (Meeson et al., 2004). The dynamic change in the relative number of cells expressing Abcg2 coincides with the timing of both the inflammatory response and myoblast expansion.

Muscle regeneration is impaired in Abcg2$^{-/-}$ mice

Cells exhibiting the potential to generate myonuclei upon intramuscular transplantation have previously been identified in the muscle SP (Asakura et al., 2002; Tanaka et al., 2009). Additionally, Abcg2 is an important determinant of the SP phenotype, and muscle SP cells are lost in Abcg2-null (Abcg2$^{-/-}$) mice (Zhou et al., 2001, 2002). These data together with the observation that Abcg2-positive cells increase significantly upon muscle injury suggest an important function for Abcg2 during muscle regeneration. Therefore, we tested the functional consequence of Abcg2 loss during skeletal muscle regeneration by assessing regeneration of the TA muscle after injury with 1.2% $BaCl_2$. Before injury, we observed no significant histological defects in the TA muscle of Abcg2$^{-/-}$ mice (Fig. 2 A). Regeneration appears delayed in Abcg2$^{-/-}$ mice at 3 and 5 d after injury. Although Abcg2$^{-/-}$ mice appear to recover 12 d after injury, the persistence of small myofibers suggests that regeneration of new myofibers is still underway (Fig. 2 A). By 30 d after injury, the overall tissue architecture is restored, whereas the number of centrally nucleated myofibers, a hallmark of regeneration, as well as the total number of myonuclei in the TA muscle of Abcg2$^{-/-}$ mice is reduced compared with wild-type littermates (Fig. 2, B and C). On average, 60% of myofibers in Abcg2$^{-/-}$ injured muscles are centrally nucleated compared with 84% of centrally nucleated myofibers in injured muscles of wild-type mice. A significant number of smaller caliber myofibers remain, whereas large myofibers are lost in Abcg2$^{-/-}$ muscle (Fig. 2 D), as demonstrated by the a reduced mean myofiber cross-sectional area of 1,627 μm^2 in Abcg2$^{-/-}$ TA muscles compared with 2,407 μm^2 in wild-type TA muscles. Fewer centrally nucleated myofibers and smaller myofiber area in Abcg2$^{-/-}$ mice indicate impaired muscle regeneration.

To further understand the regeneration defects in Abcg2$^{-/-}$ mice, we assessed the expression of embryonic myosin heavy chain (MyHC; eMyHC) as an indicator of early myogenesis and the extent of BrdU uptake to indicate the proliferation status of cells at 5 d after $BaCl_2$-induced injury. Fewer eMyHC-positive myofibers are present in Abcg2$^{-/-}$ muscle compared with wild-type muscle (Fig. 3 A). In Abcg2$^{-/-}$ mice, fewer cells have incorporated BrdU into their DNA (51 compared with 75 BrdU-positive cells per field), indicating that fewer cells are proliferating (Fig. 3, B–D). Interestingly, BrdU-positive nuclei found within laminin-positive regenerating myofibers (intralaminar) compared with extralaminar BrdU-positive cells are more greatly reduced in Abcg2$^{-/-}$ muscle than wild-type muscle, indicating that proliferation of myogenic cells is more significantly affected than nonmyogenic cells (Fig. 3 D). This decrease in cycling myogenic cells is consistent with the decrease in the total number of myonuclei observed at 30 d after injury (Fig. 2 C). Furthermore, although the number of Pax7+ satellite cells found under the basal lamina is similar in uninjured mice, 30% fewer Pax7+ satellite cells are observed at 30 d after injury in the muscle of Abcg2$^{-/-}$ mice compared with wild-type mice (Fig. 3 E). The loss of Pax7+ cells at 30 d after injury suggests a decreased ability to replenish the satellite cell pool in Abcg2$^{-/-}$ mice.

A possible mechanism leading to the regeneration defects and loss of satellite cells we observe in Abcg2$^{-/-}$ muscle is an inherent defect in the ability of satellite cells to undergo myogenesis in response to injury. To test this possibility, we isolated satellite cells from the hind limbs of Abcg2$^{-/-}$ and wild-type littermate mice and assayed their myogenic potential in vitro. We observed no significant difference in clone size, number of Pax7- or MyoD-positive cells, or in the fusion index (Table I and Fig. S1). By 3 d in culture, 80% of myonuclei are MyoD positive, and ∼40% are in multinucleated myotubes, which increases to nearly 70% after 5 d in culture.

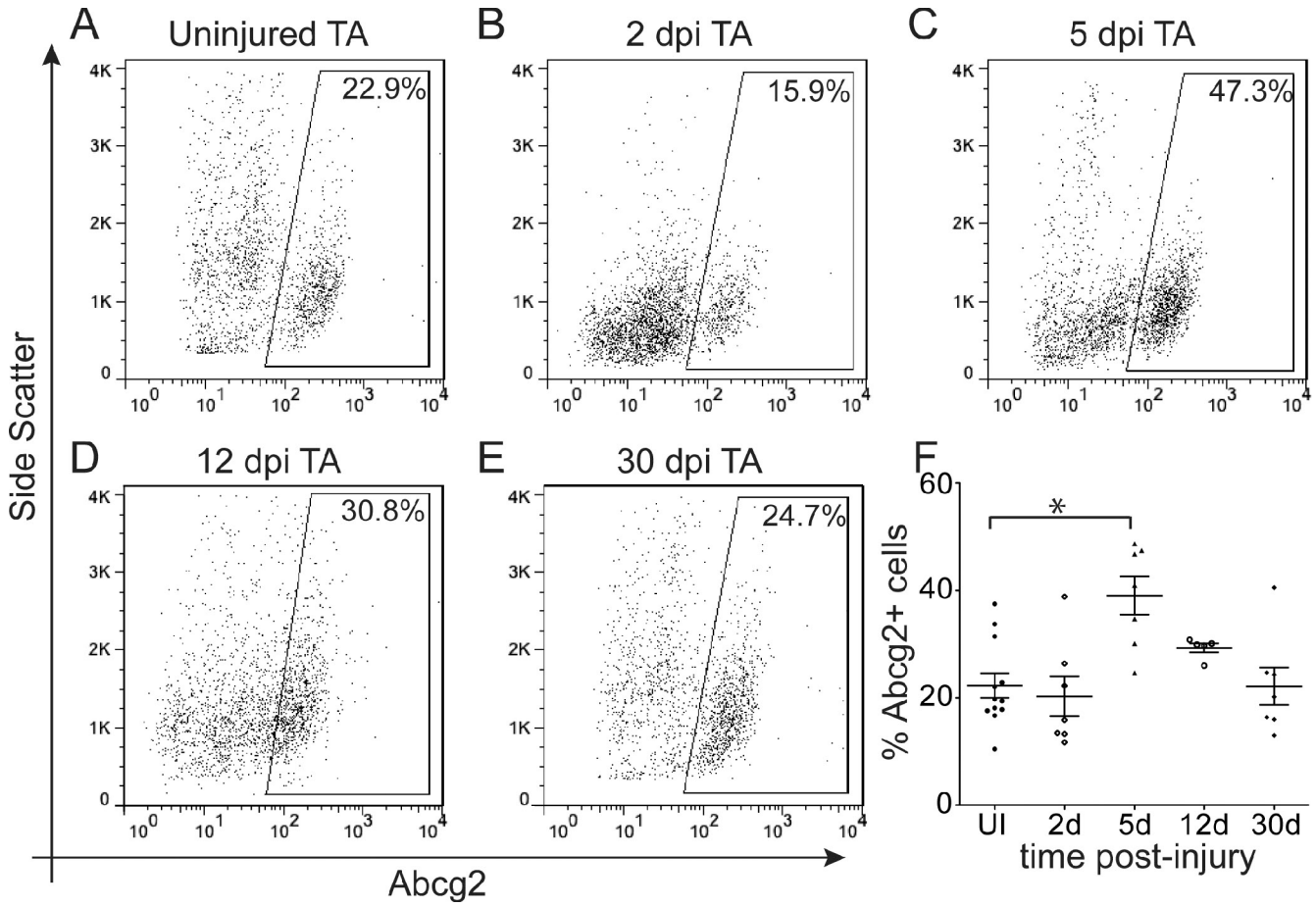

Figure 1. **Mononuclear cells expressing Abcg2 increase after $BaCl_2$-induced injury.** (A–E) Representative dot plots show Abcg2-positive cells versus side scatter with gate set to <1% false positives, isolated from uninjured (UI) TA muscle or 2, 5, 12, and 30 d postinjury (dpi) with $BaCl_2$. (B and F) Cells expressing Abcg2 peak at 5 days after injury (*, $P < 0.01$). Boxed regions indicate the percentage of cells positive for Abcg2. (F) Graph shows the mean percentages ± SEM of Abcg2-positive cells for each time point analyzed (minimum of five mice per time point).

Together, these data indicate that satellite cells isolated from $Abcg2^{-/-}$ mice proliferate and differentiate at rates similar to wild-type cells, and therefore, the satellite cells show no detectable cell-autonomous defects.

Abcg2 labels interstitial cells in skeletal muscle

Because we did not observe cell-autonomous defects in satellite cells, yet the percentage of Abcg2-expressing cells increases upon injury, we used genetic lineage tracing to identify cell progeny that arise from Abcg2-marked cells within skeletal muscle. To genetically lineage trace Abcg2-positive cells, we used a tamoxifen-inducible Cre-lox reporter system to label and follow the progeny of Abcg2-positive cells. A targeted knockin mouse expressing the Cre recombinase ER ligand binding domain fusion protein (CreERT2) from the Abcg2 locus was generated by inserting an internal ribosomal entry site–CreERT2 construct into the 3′ untranslated region of the endogenous Abcg2 gene, resulting in expression of wild-type Abcg2 and the CreERT2 fusion gene (unpublished data). $Abcg2^{CreERT2}$ mice were crossed with 129S-Gt(Rosa)26Sor^{tm1Sor}/J mice (referred to as R26R), which carry the LacZ reporter gene downstream of a loxP-flanked stop codon (Soriano, 1999). Activity of the CreERT2 fusion protein can be temporally controlled using systemically delivered tamoxifen. Adult $Abcg2^{CreERT2}$;R26R mice were treated with tamoxifen for a consecutive 3 d, and uninjured TA muscles were analyzed for expression of the β-galactosidase reporter protein at 6, 14, or 30 d after tamoxifen treatment. β-galactosidase activity is detected in a small number of interstitial cell types at 6 d after treatment (Fig. 4, A and E). The number of labeled cells increases at 14 d and reaches a peak at ∼30 d after tamoxifen treatment in uninjured muscle (Fig. 4, B, C, and E). In the TA muscle of untreated mice, no β-galactosidase activity was detected (Fig. 4 D). In uninjured muscle, we did not detect β-galactosidase staining in muscle fibers. Costaining for β-galactosidase and laminin on muscle sections showed that β-galactosidase–positive cells are excluded from the myofibers, confirming that interstitial cells are labeled by Abcg2 lineage tracing (Fig. 4 F). The increase in labeled cells over time after tamoxifen treatment suggests that Abcg2 labels a cell population in uninjured muscle that subsequently proliferates and contributes significantly to muscle interstitial cell types.

Because regeneration is impaired in $Abcg2^{-/-}$ muscle after $BaCl_2$-induced injury, and Abcg2 expression has been correlated with progenitor cells capable of forming myotubes

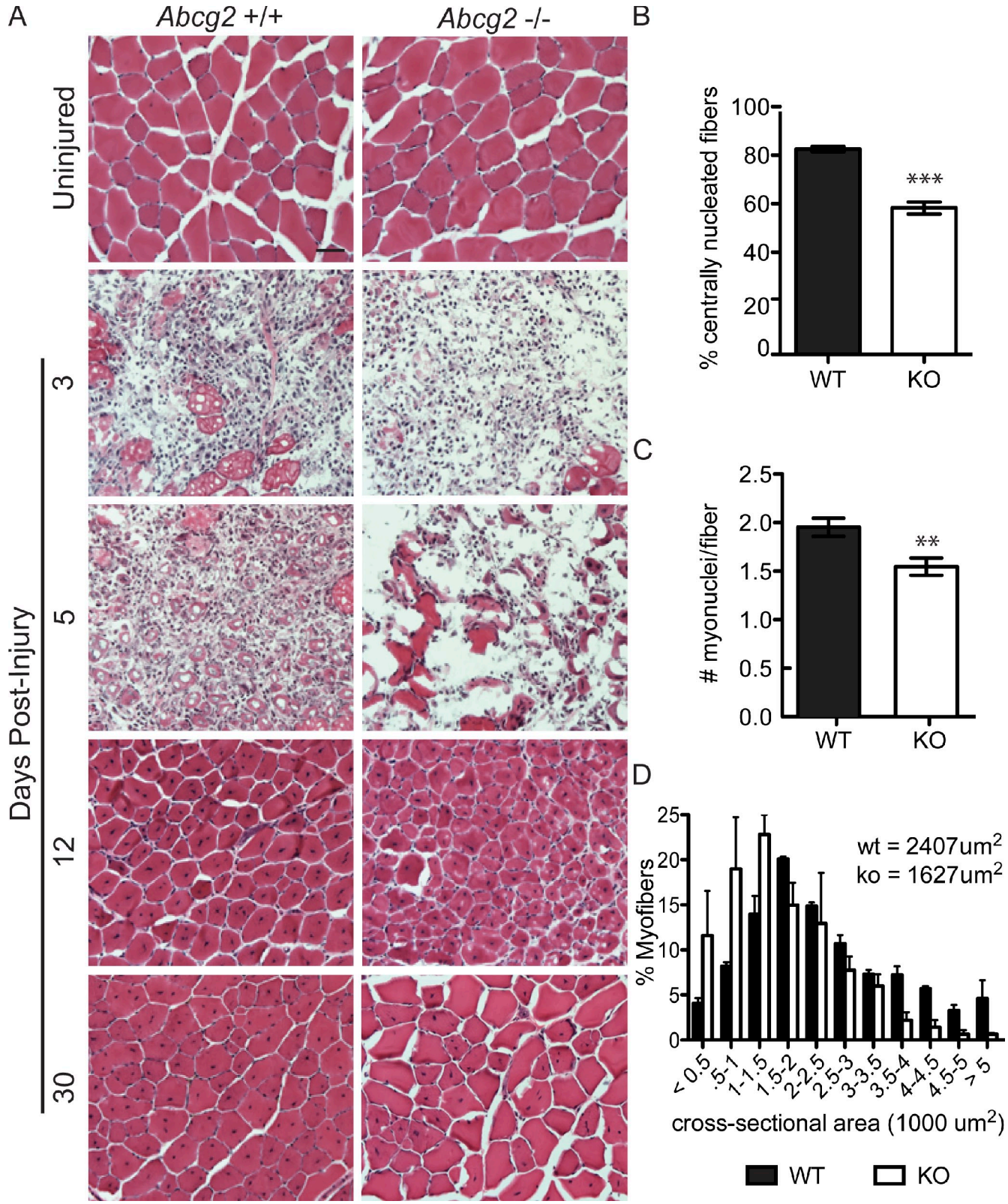

Figure 2. **Regeneration is impaired in Abcg2$^{-/-}$ mice compared with wild-type mice.** (A) Hematoxylin and eosin staining of uninjured TA muscles and TA muscles harvested at 3, 5, 12, and 30 d after injury. Hematoxylin and eosin–stained sections show delayed regeneration (day 3 and 5), fewer centrally nucleated myofibers (day 5 and 30), and reduced fiber size (day 12 and 30) in Abcg2$^{-/-}$ muscle. Bar, 50 µm. (B–D) Quantification of the reduced number of centrally nucleated myofibers (***, $P < 0.001$; B), reduced total myonuclei per fiber (**, $P = 0.0019$; C), and reduced myofiber area (D) at 30 d after injury are shown; mean cross-sectional area for wild-type (WT) myofibers is 2,407 µm^2 and Abcg2$^{-/-}$ myofibers is 1,627 µm^2 ($P < 0.001$). All values are means ± SEM. A minimum of 500 myofibers and three sections were analyzed for three mice per genotype. KO, knockout.

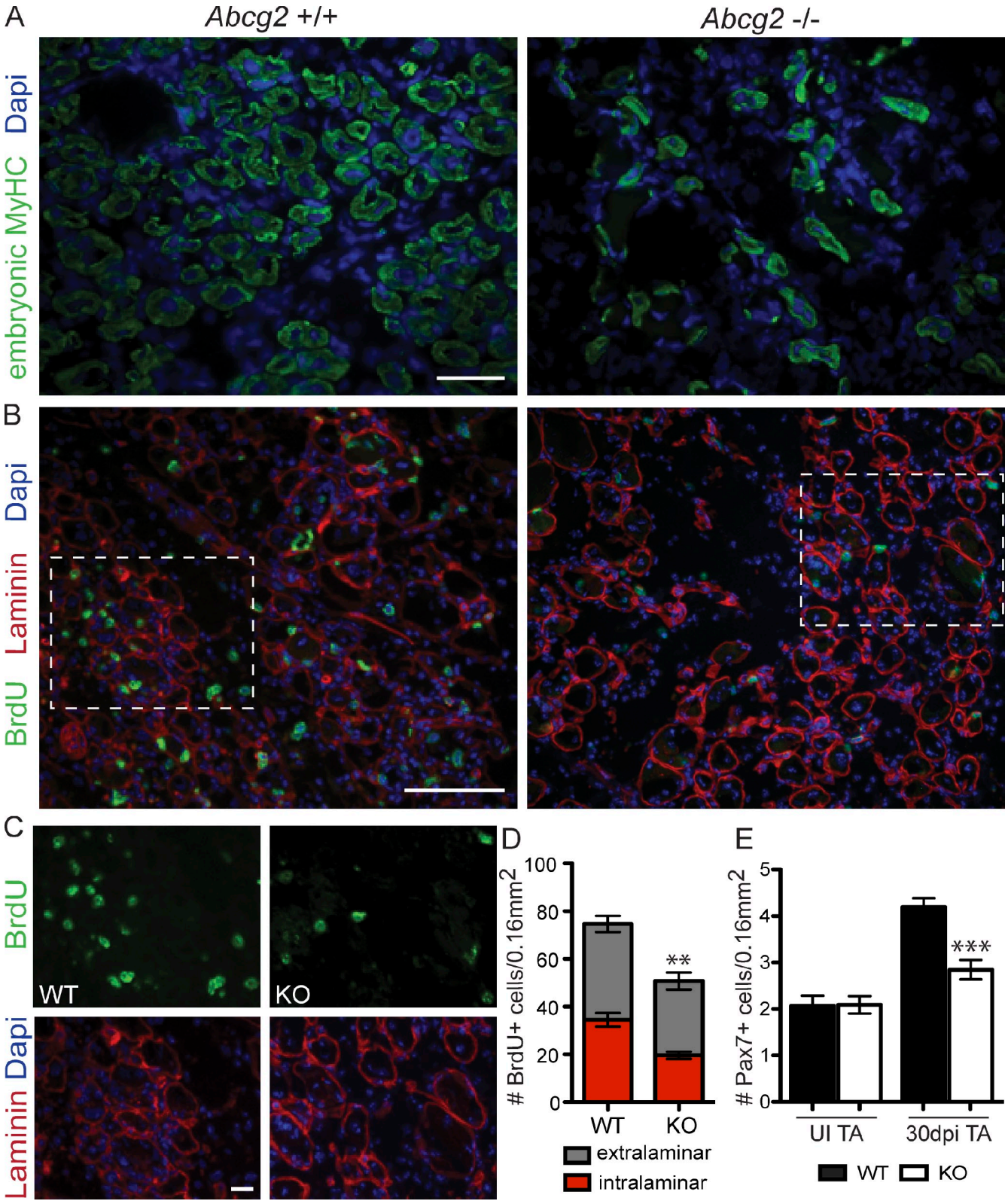

Figure 3. **Myogenesis and cell proliferation is disrupted in Abcg2$^{-/-}$ mice.** (A and B) Fewer eMyHC-expressing myofibers (green; A) and fewer BrdU-positive cells (green; B) are found in Abcg2$^{-/-}$ muscles at 5 d after injury compared with wild-type (WT) muscles. Bars, 50 µm. (C) Magnification of boxed regions in B. Bar, 10 µm. Nuclei are stained with DAPI. (D) The number of BrdU-positive cells per field is shown as means ± SEM for intralaminar (within laminin-positive regenerating myofibers; **, $P < 0.01$), extralaminar ($P = 0.4$), and total BrdU-positive cells (**, $P < 0.01$). $n = 3$ mice per genotype. (E) The number of Pax7-positive sublaminar cells per field is shown for uninjured (UI) and 30 d after injury TAs (***, $P < 0.001$ at 30 d postinjury [dpi]). Means ± SEM; $n = 4$ mice per genotype. KO, knockout.

Table I. **Abcg2$^{-/-}$ satellite cells exhibit no cell-autonomous defects**

Genotype	Colony size	Pax7+ cells	MyoD+ cells	Fusion index	
	Day 2	Day 3	Day 3	Day 3	Day 5
	Number of cells	*%*	*%*	*%*	*%*
Abcg2$^{+/+}$	41 ± 5	57.9 ± 3.6	78.2 ± 3.0	39.0 ± 2.6	65.7 ± 2.2
Abcg2$^{-/-}$	33 ± 4	48.8 ± 3.7	83.9 ± 2.6	36.9 ± 2.1	67.6 ± 2.2

The number of nuclei in multinucleated MyHC-positive myotubes per total myonuclei was scored (fusion index). Values are means ± SEM. *n* = 3 independent experiments.

in vitro under some conditions and contributing to myofiber regeneration upon transplantation into injured muscle (Meeson et al., 2004; Tanaka et al., 2009), we reasoned that Abcg2 progeny would contribute to newly formed myofibers after injury. To test this hypothesis, we injured Abcg2^{CreERT2};R26R mice with 1.2% $BaCl_2$ at various time points relative to tamoxifen injection and assessed the contribution of β-galactosidase–positive cells to regenerated myofibers at 30 d after injury. In the uninjured TA muscle 30 d after tamoxifen treatment, no β-galactosidase staining is detected in myofibers (Fig. 5 A and Fig. 4 C). Although an induced injury performed 14 d after tamoxifen treatment yielded no detectable β-galactosidase staining in regenerated (centrally nucleated) myofibers (Fig. 5 B), an injury induced concurrently with tamoxifen treatment (at the time of the second tamoxifen injection) yielded detectable β-galactosidase activity in a small number of regenerated myofibers (Fig. 5 C and Fig. S2 B). We observed clusters of 1–8 positive myofibers in the TA muscle of 5 out of 11 mice injured concurrently with tamoxifen treatment. The punctate staining pattern we observe is consistent with the cytoplasmic localization of the LacZ gene when low levels of LacZ are expressed from the Rosa locus and similar to the staining pattern observed in muscle fibers of Actin^{CreERT2};R26R mice upon low levels of Cre-mediated recombination (Fig. S2 B). These results demonstrate that endogenous Abcg2-labeled cells can contribute to myofibers, but this contribution is minor in vivo using our injury/labeling procedure. Interestingly, Abcg2 marks ∼60% of interstitial cells regardless of whether the TA muscle was injured or when it was injured relative to tamoxifen treatment (Fig. 5 E). Furthermore, when we bred Abcg2^{CreERT2};R26R to the mdx^{4cv} mouse (mouse model of

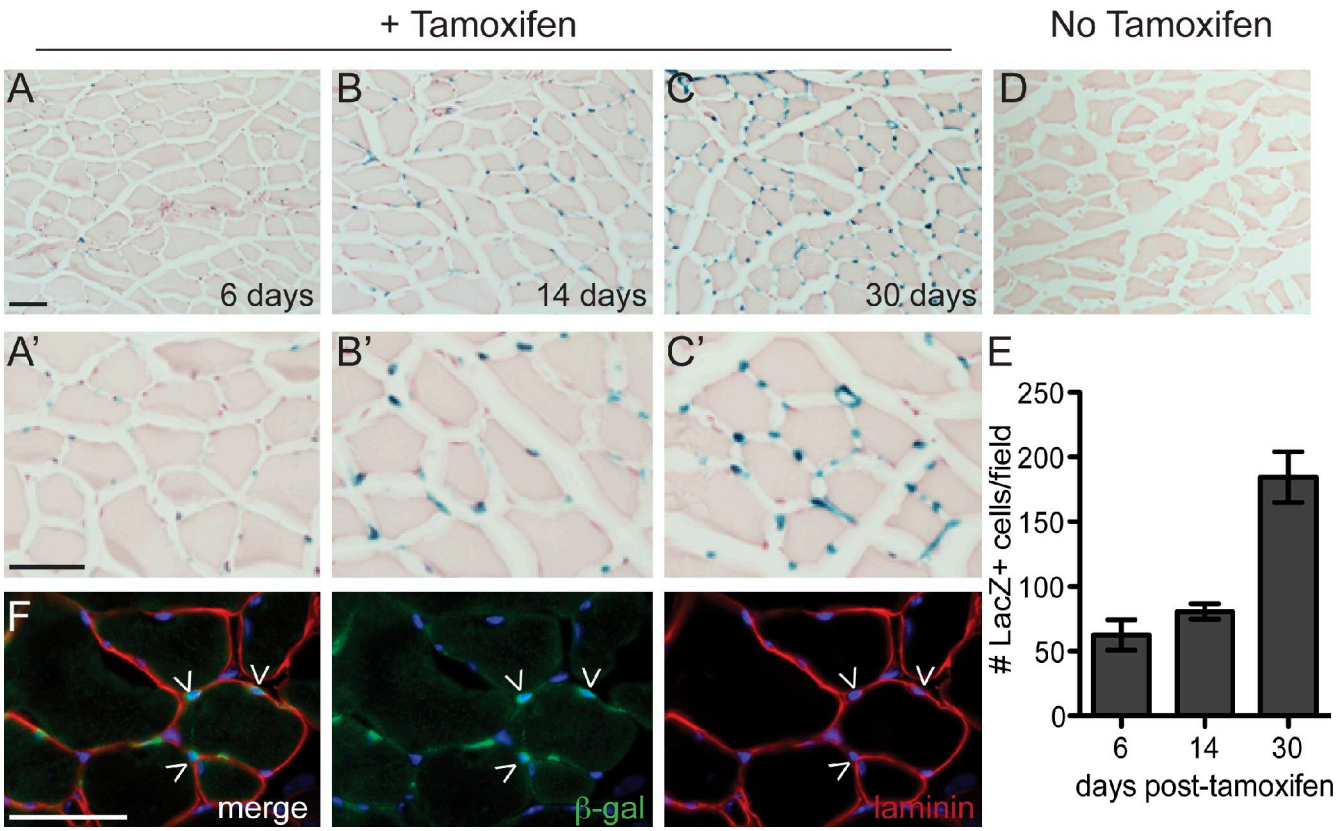

Figure 4. **Interstitial cell types are labeled by an Abcg2-driven CreERT2 and increase over time.** (A–C) X-gal staining of uninjured TA muscles at 6 d (A), 14 d (B), and 30 d (C) after tamoxifen treatment show labeling of interstitial cells that increase over time. (D) TA muscle sections from untreated mice show no detectable X-gal staining. (A′–C′ and E) Magnification of A–C (A′–C′) and quantification of β-galactosidase (β-gal)–positive cells (E) are shown. Means ± SEM; *n* = 3 mice per time point. (F) Immunoreactivity of β-galactosidase and laminin antibodies confirms that labeled cells are excluded from the myofiber. Nuclei are stained with DAPI (blue). Arrowheads indicate β-galactosidase–positive cells. Bars, 50 µm.

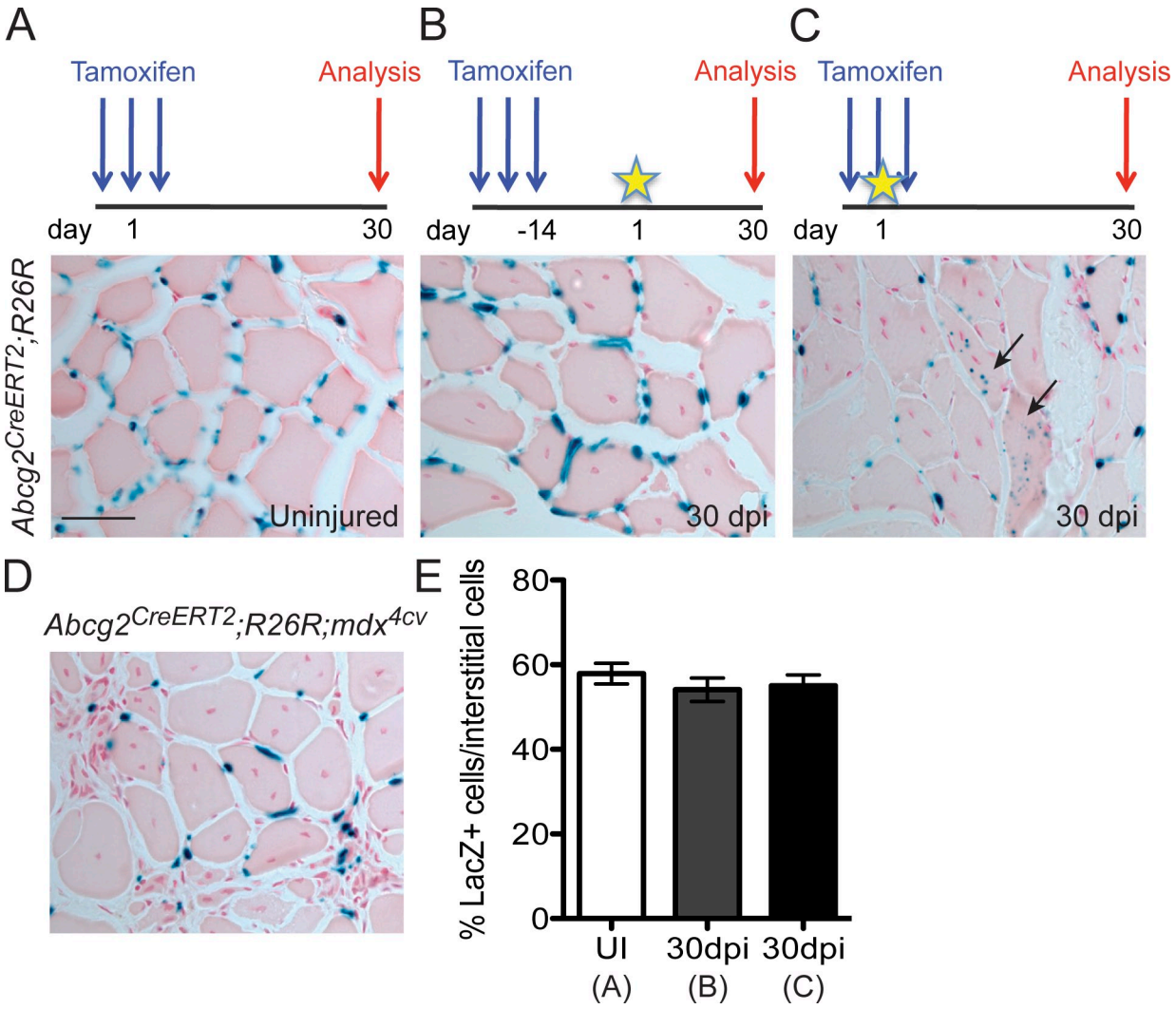

Figure 5. **Abcg2 progeny do not contribute significantly to myofiber regeneration.** (A–C) X-gal staining of tissue sections from uninjured TA muscle 30 d after tamoxifen treatment (A), 30 d postinjury (dpi) TA muscle injured 14 d after tamoxifen treatment (n = 10; B), or during tamoxifen treatment (n = 11; C). Arrows indicate two fibers with punctate β-galactosidase staining. (C) 1–8 positive myofibers per section in five of 11 mice analyzed are β-galactosidase positive. (D) TA muscle from Abcg2^{CreERT2};R26R mice crossed to mdx^{4cv} mice show no β-galactosidase–positive myofibers (n = 4). Schematic shows time line of tamoxifen treatment, injury time point, and time of analysis. The time of injury is indicated as day 1 (stars in B and C). (E) The number of β-galactosidase–positive cells as a percentage of total interstitial cells is shown as mean percentage ± SEM for uninjured (UI; bar A), 30 dpi injured at 14 d after tamoxifen treatment (gray bar; bar B), or 30 d after injury injured during tamoxifen treatment (black bar; bar C) TA muscles (n = 3 mice per condition). Bar, 50 µm.

Duchenne muscular dystrophy; Im et al., 1996), we did not detect contribution from Abcg2-labeled cells to myofibers in the mdx^{4cv} mouse (Fig. 5 D), suggesting Abcg2-labeled cells do not contribute directly to muscle regeneration in a model of chronic muscle damage.

Abcg2 progeny include multiple interstitial cell types

Cells located in the interstitium include several cell types that either possess myogenic potential or indirectly and positively regulate myogenesis (Péault et al., 2007; Abou-Khalil et al., 2010). Among these cells are vascular-associated cells, including endothelial cells and pericytes, FAPs, muscle SP cells, and PW1+/Pax7− interstitial cells (Asakura et al., 2002; Tamaki et al., 2002; Meeson et al., 2004; Dellavalle et al., 2007; Joe et al., 2010; Mitchell et al., 2010; Uezumi et al., 2010). Because Abcg2-marked cells predominately contribute to interstitial cells, and satellite cell–derived cultures from Abcg2$^{-/-}$ mice display no detectable defects, yet regeneration is impaired in Abcg2$^{-/-}$ mice, we hypothesized that Abcg2-marked interstitial cells indirectly support myogenesis. To better understand which cell types are labeled by Abcg2, we undertook a thorough analysis of the cells marked by Abcg2 lineage tracing in uninjured muscle. Our previous analysis indicated that many cells coexpress Abcg2 and Sca-1 (stem cell antigen 1), so we assessed the expression of Sca-1 within Abcg2-labeled progeny. Sca-1 is widely expressed by progenitor populations in multiple tissues and many muscle interstitial cell types, including FAPs and CD31-positive endothelial cells (Tamaki et al., 2002; Mitchell et al., 2005; Joe et al., 2010). By immunofluorescence using anti–β-galactosidase antibodies, β-galactosidase is widely colocalized in cells expressing Sca-1 (Fig. 6 A) as

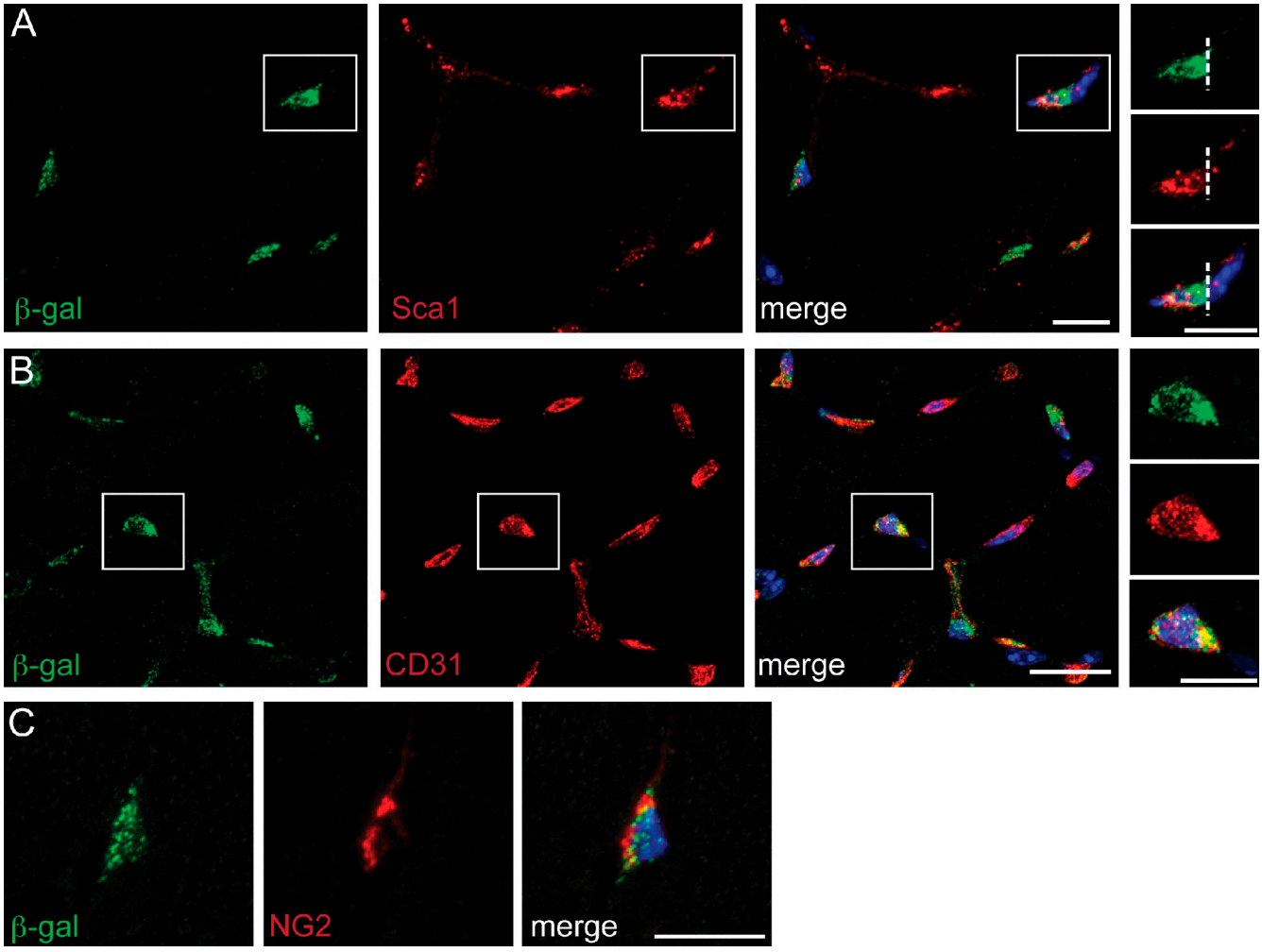

Figure 6. **β-galactosidase expression colocalizes with markers of vascular-associated cells.** (A–C) Confocal microscopy (z projections of eight focal planes) demonstrates that β-galactosidase (β-gal) colocalizes in cells with Sca-1 (A), CD31 (B), and NG2 (C). Nuclei are stained with DAPI (blue). (A and B) Insets show enlarged images of boxed regions. Note that in A, there are two cells marked by the dashed lines; the right cell is negative for both β-galactosidase and Sca-1. Bars, 10 µm.

well as in endothelial cells expressing the cell surface antigen CD31 (Pecam-1; Fig. 6 B). We also observe colocalization of β-galactosidase with the proteoglycan NG2, a marker of pericytes (Fig. 6 C; Dellavalle et al., 2007).

To quantify this coexpression, we took advantage of the fluorescent β-galactosidase substrate fluorescein di-β-D-galactopyranoside (FDG) to label Abcg2 progeny for analysis by flow cytometry. At 2 wk or longer after tamoxifen treatment, ∼25% of mononuclear cells from uninjured hind-limb muscles are FDG positive (Fig. 7 A). In uninjured muscle, CD31-positive endothelial cells comprise >80% of FDG-positive cells (Fig. 7 B and Table II). The majority of these cells are also positive for the cell surface markers Sca-1 and α7-integrin (Fig. 7 C). We further considered the minority of FDG-positive cells that are negative for CD31 (Fig. 7 B). Myogenic cells have been characterized as α7-integrin positive and/or CD34 positive within in the CD31-negative and Sca-1–negative fraction (Montarras et al., 2005; Sacco et al., 2008; Joe et al., 2010). Based on this combination, <1% of FDG-positive cells are myogenic progenitors (Fig. 7, D and F; and Table II). Recently, adipogenic progenitors and FAPs found in muscles have been reported (Joe et al., 2010; Uezumi et al., 2010). We determined that although the majority of FDG-positive and CD45 and CD31 double-negative cells express PDGF-R-α, few are also positive for Sca-1, indicating that <1% of total FDG-positive cells are FAPs (Fig. 7 E and Table II).

Abcg2 is expressed by stem cells in bone marrow as well as skeletal muscle (Zhou et al., 2001), and bone marrow cells positive for CD45 (a hematopoietic cell lineage marker) have been shown to traffic to skeletal muscle (Rivier et al., 2004). Therefore, we determined whether Abcg2 progeny were CD45 positive and observed that <10% of FDG-positive cells are also positive for CD45 in uninjured muscle (Fig. 7 F and Table II). Within the FDG-positive, CD45-negative fraction of cells, ∼20% are Sca1 and CD34 double positive. It remains unclear what this small fraction of cells exactly is, as expression of Sca-1 and CD34 has been associated with numerous progenitor populations, including muscle SP cells, muscle-derived stem cells, and myoendothelial cells (Tamaki et al., 2002; Péault et al., 2007). Together, these data suggest

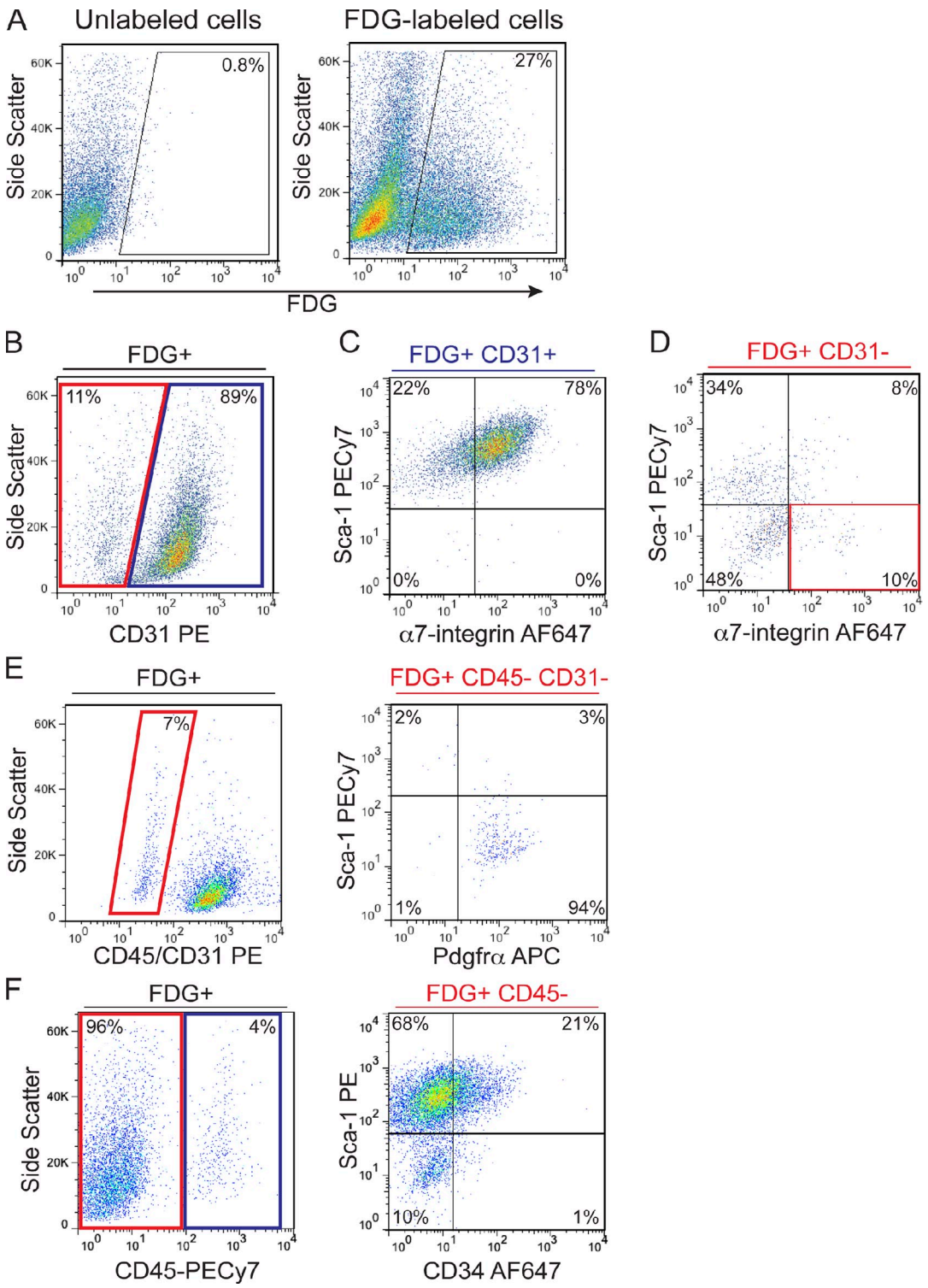

Figure 7. **β-galactosidase–positive cells coexpress markers of muscle interstitial cell types.** FDG was used to label live cells expressing β-galactosidase isolated from hind-limb muscles followed by staining with fluorophore-conjugated antibodies for analysis by flow cytometry including Sca-1, CD31, α7-integrin, CD45, CD34, and PDGF-R-α. (A) Approximately 25% of cells detected from Abcg2^{CreERT2};R26R mice treated with tamoxifen are FDG+ (A, gated region). Less than 1% of cells isolated from mice that had not received tamoxifen are FDG+ (gated region) similar to unlabeled cells. Analysis of FDG coexpression with various markers was performed by first gating for FDG and then the antibody of interest and are shown as described at the bottom. Gates are set to <1% positives on appropriate fluorescence minus one controls. (B) The majority of FDG+ cells are positive for the endothelial cell marker CD31 (blue box). (C) FDG+ and CD31+ (blue box in B) cells are gated onto a plot for α7-integrin versus Sca-1, showing that most CD31+ cells are also α7-integrin+ and Sca-1+ (C, top right quadrant). (B and D) Similarly, FDG+ and CD31− (11%, red box in B) cells are gated onto a plot for α7-integrin versus Sca-1 showing 10% myogenic (α7-integrin+ and Sca-1−) cells (red box in D), indicating <1% of FDG+ cells are myogenic. (E) The CD45/CD31− (7%, red box) fraction of FDG+ cells was gated onto a plot for PDGF-R-α versus Sca-1, which shows most of these cells are PDGF-R-α+ and Sca-1−. (F) CD45+ cells make up <10% of FDG+ cells (blue box). The FDG+ and CD45− fraction (red box) is gated for CD34 versus Sca-1, which shows that ~20% are CD34+ and Sca1+ and may include other progenitor populations but few myogenic cells (CD34+ and Sca-1−). Dot plots shown are representative of three to six independent experiments. APC, allophycocyanin; PE, phycoerythrin.

Table II. **Abcg2-labeled cell populations in uninjured skeletal muscle**

Cell type	Markers	FDG+ cells
		%
Endothelial cells	CD31+, Sca1+, α7-integrin+	79 ± 5
Bone marrow–derived cells	CD45+	10 ± 2
Myogenic cells[a,b]	CD31−, Sca1−, α7-integrin+	<1
FAPs[b,c]	CD31−, CD45−, Sca1+, PDGF-R-α+	<1
Other muscle progenitor cells[d,e]	CD45−, Sca1+, CD34+	<20

Values are means ± SEM; *n* = 3–6 independent experiments.
[a]Blanco-Bose et al., 2001.
[b]Joe et al., 2010.
[c]Uezumi et al., 2010.
[d]Tamaki et al., 2002.
[e]Péault et al., 2007.

that most Abcg2 progeny are resident endothelial cells within muscle, and a small number of Abcg2 progeny are derived from the hematopoietic lineage.

Abcg2-labeled, CD45-positive cells increase upon injury

Because Abcg2-expressing cells increase upon an induced muscle injury, we further extended our study of Abcg2-labeled cells to 5 d after muscle injury to understand which cell types may be positively regulating muscle regeneration. Similar to the profiles obtained using the anti-Abcg2 antibody (Fig. 1), the percentage of mononuclear cells that are FDG positive increases at 5 d after injury and subsequently, returns to uninjured levels by 30 d after injury (Fig. 8 A). This significant increase in Abcg2-labeled progeny could represent the proliferation of cells labeled in uninjured tissue, or it could represent an influx of cells from the peripheral blood in response to injury. To test these two possibilities, Abcg2-marked cells were labeled with FDG and costained for antibodies of interest at 5 d after muscle injury and then analyzed by flow cytometry. Compared with uninjured TA muscles, the relative percentage of CD31- and Sca-1–positive endothelial cells within FDG-positive cells decreased in injured muscle (Fig. 8 B). However, the majority of FDG-positive cells at 5 d after injury were immunoreactive for CD45 and negative for Sca-1 (Fig. 8 C). CD45 and Sca-1 double-positive resident muscle cells increase upon injury (Polesskaya et al., 2003), whereas bone marrow–derived CD45-positive cells have been shown to traffic to skeletal muscle after injury (Rivier et al., 2004). We hypothesized that the influx of FDG and CD45 double-positive cells upon injury are derived from a lineage originating in the bone marrow not a resident muscle lineage, as they are negative for Sca-1. Because the inflammatory response precedes and supports myogenesis, we reasoned that some of the Abcg2-labeled, bone marrow–derived cells may be macrophages (Arnold et al., 2007; Tidball and Wehling-Henricks, 2007; Tidball and Villalta, 2010). Thus, we asked whether the muscle injury-induced, Abcg2-labeled cells included macrophages. At 5 d after injury, we detected coexpression by immunofluorescence of the Abcg2-responsive reporter gene β-galactosidase and the macrophage marker F4/80 (Fig. 8 D). Therefore, the transient increase in Abcg2-labeled cells in injured muscle tissue likely derives from circulating hematopoietic cells. Collectively, our data suggest that Abcg2-marked cells in muscle include a population of resident interstitial cells (CD45 negative in uninjured tissue) and a population of circulating cells that traffic to the muscle upon injury (CD45 positive), further supporting the hypothesis that Abcg2-positive cells positively contribute to muscle regeneration.

Immune response, but not angiogenesis, is affected in Abcg2$^{-/-}$ mice upon injury

The impaired regeneration phenotype in Abcg2$^{-/-}$ mice is not explained by cell-autonomous defects in satellite cells; however, Abcg2 is expressed in muscle interstitial cells types in uninjured tissue and infiltrates cells upon injury. It is becoming appreciated that the cellular processes of angiogenesis and the inflammatory response precede myogenesis. Both of these cellular events positively regulate myogenesis (Abou-Khalil et al., 2010; Tidball and Villalta, 2010). Therefore, we examined the angiogenic and immune responses at early time points after injury in Abcg2$^{-/-}$ muscle. The density of vasculature as assessed by CD31 and vascular endothelial (VE) cadherin staining was unaffected in Abcg2$^{-/-}$ muscle at 5 d after injury (Fig. 9, A and B; and not depicted). Although there appears to be no significant defect in generation of new vasculature, signaling from endothelial cells could be impaired, so we analyzed the mRNA expression levels of several angiogenic signaling genes. We detect no differences in uninjured muscle. At 3 d after injury, VEGFa and HIF2-α remain unchanged, whereas Angiopoietin-1, Angiopoietin-2, and HIF1-α trend toward decreased expression in Abcg2$^{-/-}$ muscle (Fig. 9, C–G).

Impaired recruitment of macrophages to muscle after injury can have a negative effect on muscle regeneration (Arnold et al., 2007; Contreras-Shannon et al., 2007). The significant increase in Abcg2 expression correlates with recruitment of bone marrow–derived cells, so we determined whether the immune response to muscle injury was impacted in Abcg2$^{-/-}$ muscle. The inflammatory response is characterized by two waves of macrophage infiltration: M1 macrophages

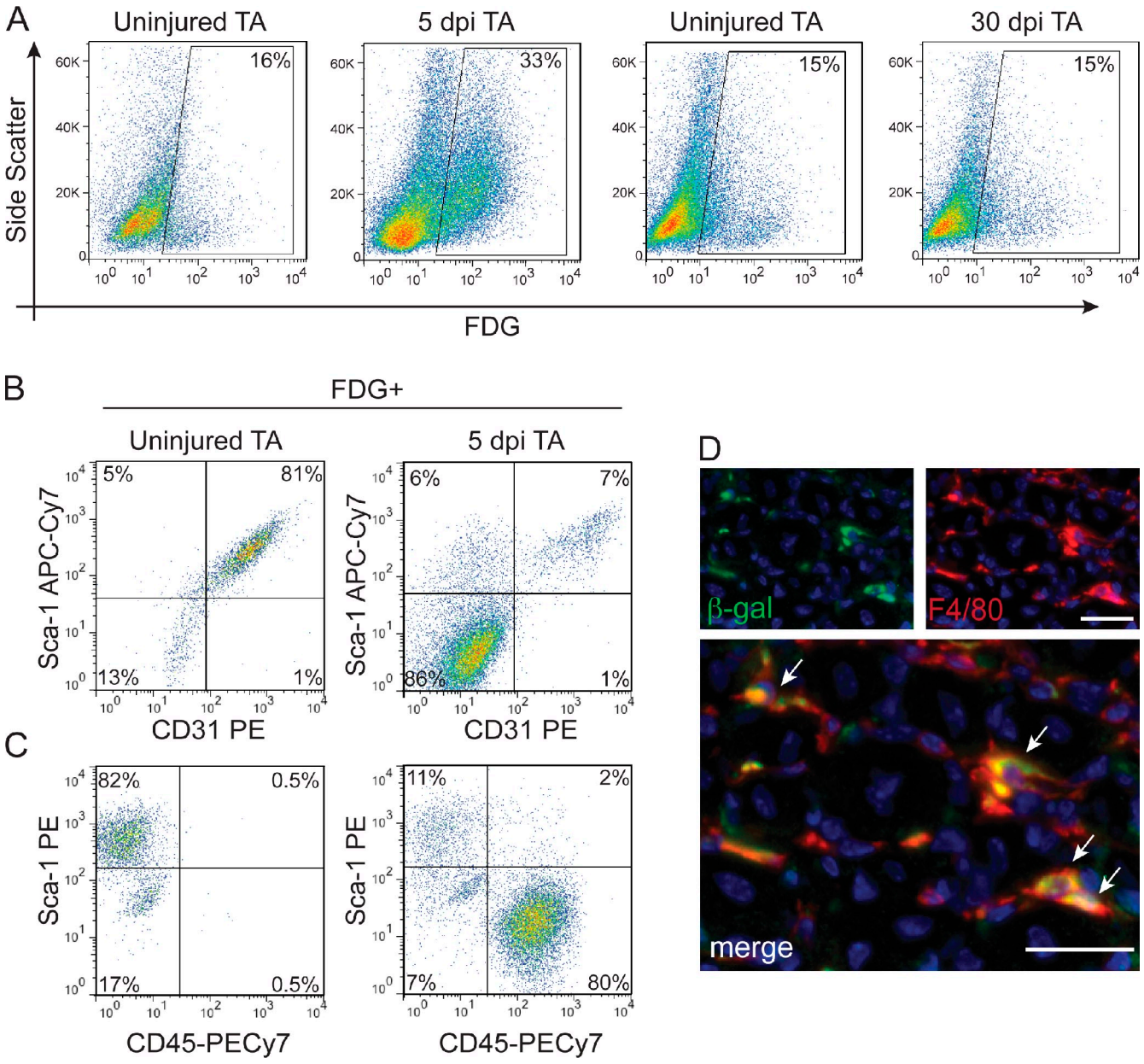

Figure 8. **Abcg2-labeled cells that are CD45 positive increase at 5 d after $BaCl_2$-induced injury.** Cells labeled with FDG were analyzed via flow cytometry. (A) Representative dot plots show FDG versus side scatter for cells isolated from injured TA muscles at 5 and 30 d postinjury (dpi) and the respective contralateral uninjured TA muscles. Gated regions indicate the percentage of FDG+ cells. (B and C) FDG+ cells from uninjured (left) and 5 d after injury TA muscles (right) were gated for CD31 versus Sca-1 (B) and CD45 versus Sca-1 (C). As a fraction of the FDG-labeled cells, endothelial cells decrease (CD31+ and Sca-1+; top right quadrant in B) and CD45+ (Sca-1−; bottom right quadrant in C) bone marrow–derived cells increase at 5 d after injury relative to uninjured control. Dot plots shown are representative of four experiments. Numbers correspond to the percentage of positive cells in the given quadrant. (D) Tissue sections from 5 d after injury TA muscle were stained for β-galactosidase (β-gal) and the macrophage marker F4/80. Arrows indicate cells that coexpress β-galactosidase and F4/80 (yellow). APC, allophyrocyanin; PE, phycoerythrin. Bars, 50 µm.

are recruited as part of a proinflammatory (Th1) response and peak at 2–3 d after injury. This is followed closely by an anti-inflammatory (Th2) response in which M2 macrophages are recruited and peak between 4 and 6 d after injury (Tidball and Villalta, 2010). We assessed the total number of macrophages during both phases. No difference in macrophage number is detected in uninjured tissue or at 3 d after injury (Fig. 10, A and C; and not depicted). However, ∼30% fewer macrophages are found in $Abcg2^{-/-}$ muscle at 5 d after injury (Fig. 10, B and C), suggesting that recruitment of antiinflammatory M2 macrophages may be negatively impacted in $Abcg2^{-/-}$ muscle. Consistent with this observation, we find that expression of TNF-α and IL-6, both proinflammatory cytokines that inhibit M2 macrophage recruitment (Zádor et al., 2001; Warren et al., 2002), trend toward increased expression in *Abcg2*$^{-/-}$ muscle (Fig. 10, D and E). Additionally, CCL2 (MCP-1), a chemotactic and activating factor for macrophages that has been shown to be important for muscle regeneration (Shireman et al., 2007), trends toward decreased expression in *Abcg2*$^{-/-}$ muscle (Fig. 10 F).

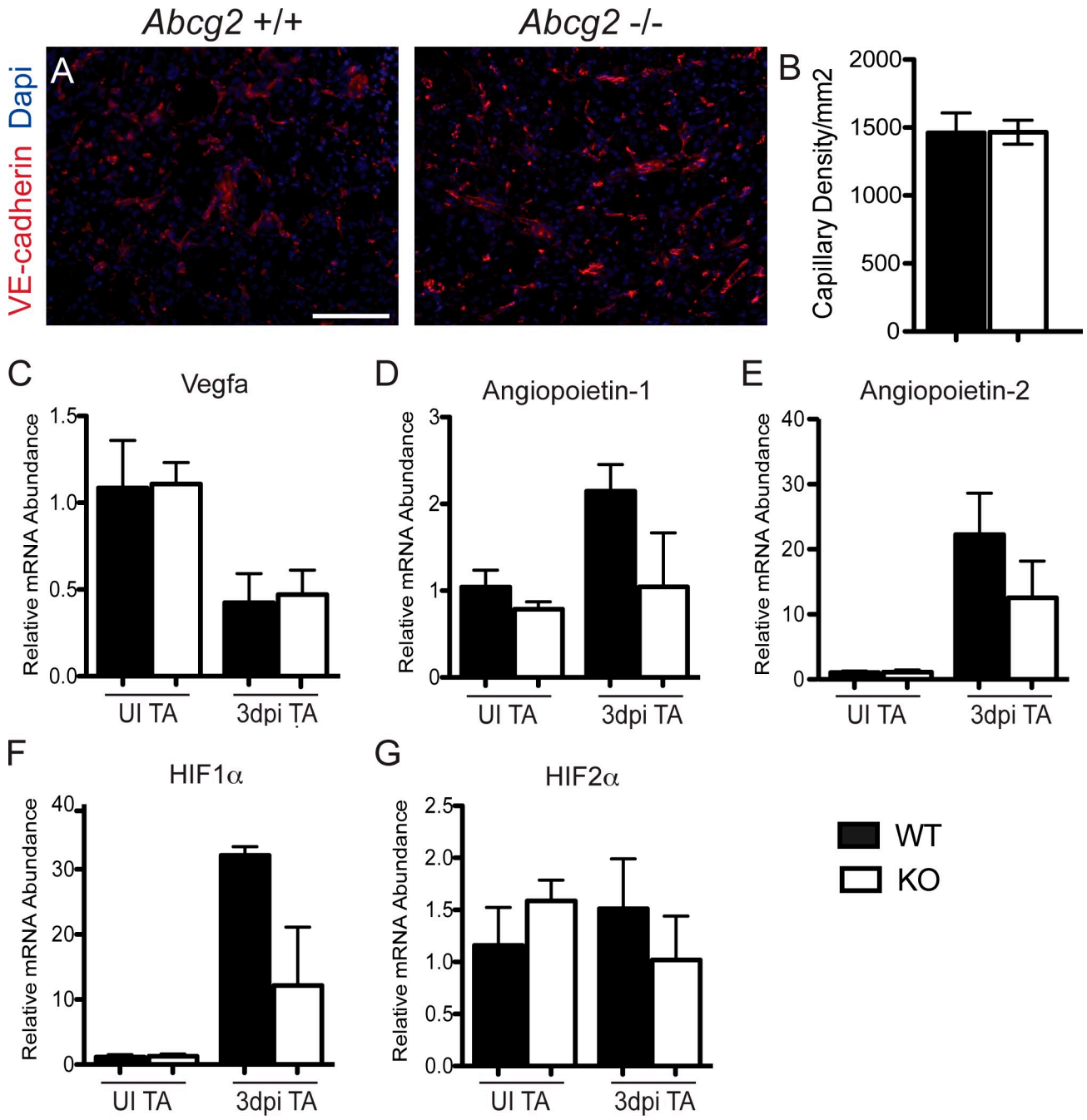

Figure 9. **Formation of new capillaries is unperturbed, but angiogenic signaling is disrupted in *Abcg2*$^{-/-}$ mice.** (A) VE-cadherin staining indicates similar capillary density between *Abcg2*$^{+/+}$ and *Abcg2*$^{-/-}$ muscle after injury. Bar, 50 µm. (B) Capillary density was determined by scoring the total positive pixel area for VE-cadherin per field. Values are means ± SEM; $n = 3$. (C–G) Quantitative RT-PCR for VEGFa (C), Angiopoietin-1 (D), Angiopoietin-2 (E), HIF1-α (F), and HIF2-α (G) was performed on RNA isolated from uninjured (UI) TA and 3 d postinjury (dpi) TA muscles ($n = 3$). WT, wild type; KO, knockout.

Discussion

Expression of the ABC transporter Abcg2 is the major molecular determinant of the SP phenotype in skeletal muscle and in other cells, including cells in the hematopoietic lineage and heart tissue (Zhou et al., 2002; Martin et al., 2004; Meeson et al., 2004). In this study, we demonstrate that upon genetic loss of Abcg2, in which SP cells are depleted, skeletal muscle regeneration is delayed. We further show that in skeletal muscle, Abcg2-marked cells give rise to multiple interstitial cell types, including endothelial cells and pericytes in uninjured tissue. Furthermore, upon muscle injury, Abcg2-expressing cells increase, and Abcg2 progeny include infiltrating cells from the peripheral blood, of which some are macrophages. The recruitment of circulating cells to muscle after injury is impaired in *Abcg2*$^{-/-}$ mice.

Abcg2 labeling gives rise to vascular-associated cells within skeletal muscle

Based on the conditional expression of the LacZ reporter gene, we show that Abcg2-marked cells generate numerous interstitial

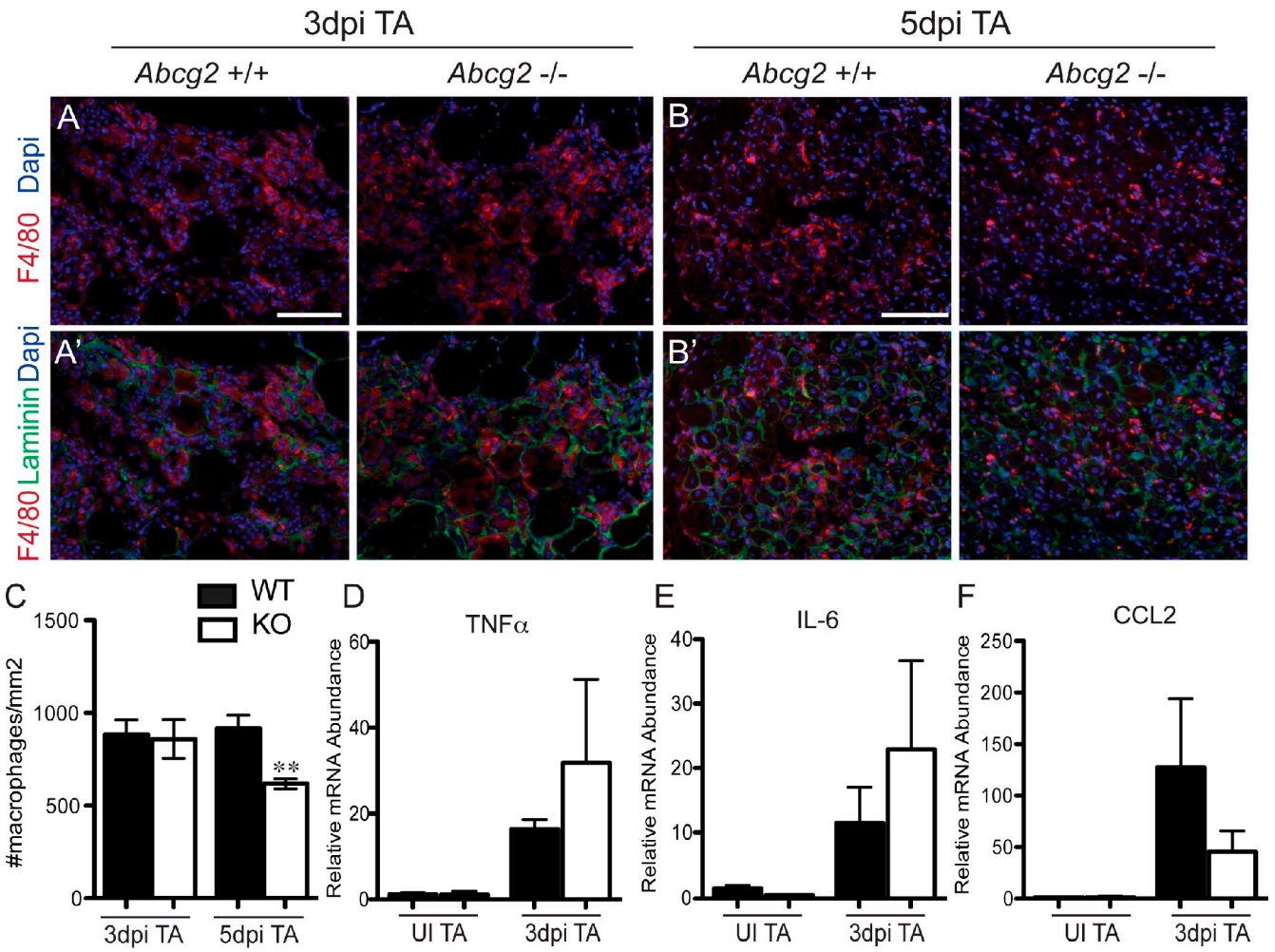

Figure 10. **The antiinflammatory immune response is disrupted in *Abcg2*$^{-/-}$ mice.** (A and B) Staining with the macrophage marker F4/80 with and without laminin is shown for tissue sections 3 d (A) and 5 d (B) after $BaCl_2$-induced injury. Bars, 50 µm. (C) Sections were scored for F4/80-positive cells. Values shown are means ± SEM; $P < 0.01$ for 5 d postinjury (dpi); $n = 3$ mice per genotype for each time point. (D–F) Quantitative RT-PCR for TNF-α (D), IL-6 (E), and CCL2 (F) was performed on RNA isolated from uninjured (UI) TA and 3 d after injury TA muscles ($n = 3$). WT, wild type; KO, knockout.

cell types in skeletal muscle. SP cells comprise 1–2% of interstitial cells within skeletal muscle. Although Abcg2 is expressed by SP cells, we find that Abcg2 progeny include 20–50% of muscle interstitial cells. Specifically, a large majority of endothelial cells and some pericytes, based on β-galactosidase coexpression with CD31 and NG2, are derived from an Abcg2-positive progenitor cell, which is consistent with the previous observation that Abcg2-positive cells are located in close proximity to the vasculature (Meeson et al., 2004). Additionally, we show expression of Sca-1 and α7-integrin with the majority of Abcg2 progeny and expression of CD34 with a minority of Abcg2 progeny. Isolated myogenic progenitor cells express both CD34 and α7-integrin (Sca-1 and CD31 negative; Beauchamp et al., 2000; Blanco-Bose et al., 2001; Montarras et al., 2005; Joe et al., 2010) and recently identified that fibrogenic and adipogenic progenitors express PDFG-R-α and Sca-1 (CD45 and CD31 negative; Joe et al., 2010; Uezumi et al., 2010). Based on these markers, we find that few myogenic progenitors or FAPS are derived from *Abcg2* progeny. We do find that a small population of *Abcg2*-derived cells is positive for CD34 and Sca-1 (CD45 negative), which likely includes SP cells and possibly, other muscle-derived stem cells or myoendothelial cells (Tamaki et al., 2002; Zheng et al., 2007; Péault et al., 2007).

Upon injury, we observe a significant increase in the percentage of Abcg2-labeled cells. Unlike in uninjured tissue in which the majority of labeled cells are CD45 negative, upon injury, the majority of Abcg2 progeny are CD45 positive. Furthermore, a subset of Abcg2 progeny is positive for the macrophage marker F4/80. Upon injury, bone marrow–derived cells, including circulating monocytes, which differentiate into macrophages, are recruited to the muscle where they participate in the inflammatory process and promote regeneration (Rivier et al., 2004; Arnold et al., 2007). Hematopoietic lineage progenitors also express Abcg2; therefore, it is possible that the observed increase in Abcg2-positive cells upon injury results from circulating cells infiltrating the muscle tissue. In support of this hypothesis, circulating cells derived from hematopoietic stem cells are labeled by Abcg2. Using a conditional Rosa26-YFP reporter, YFP is detected in circulating cells expressing GR1 and Mac1, surface antigens of monocytes (unpublished data).

Based on these observations, we propose that Abcg2 labels two distinct populations of cells: (1) resident muscle interstitial cells and (2) circulating progenitor cells that traffic to skeletal muscle upon injury.

Abcg2+ cells are not a significant source of myogenic progenitors

Previous studies have proposed that SP cells prospectively isolated from skeletal muscle possess myogenic activity and thus, may either contribute to renewal of the satellite cell population or may be an independent progenitor cell (Asakura et al., 2002; Tanaka et al., 2009). Our lineage tracing data using the Abcg2 locus to drive expression of CreERT2 suggests that Abcg2-labeled cells possess limited myogenic activity. A few possibilities may account for the low contribution of Abcg2 labeling to new myofibers in our study. (a) Prior studies demonstrated the ability of isolated SP cells to contribute to generation of new myofibers upon intramuscular transplantation (Asakura et al., 2002; Meeson et al., 2004). The manipulation of isolated cells for transplantation may alter the properties of SP cells such that they can undergo myogenic differentiation. Alternatively, the transplant procedure could give the SP cells a competitive advantage over endogenous satellite cells. (b) The Abcg2-labeled cells that contribute to myofibers may come from bone marrow cells. Previous studies have shown that bone marrow–derived cells, including SP cells, differentiate to myogenic cells at a low frequency (Ferrari et al., 1998; Gussoni et al., 1999; Ojima et al., 2004; Luth et al., 2008). These observations are consistent with the low Abcg2 labeling of regenerated myofibers we detect when injuries are performed concurrently with tamoxifen treatment such that the Abcg2 and CD45 double-positive cells are also labeled. (c) The level of CreERT2 expression from the Abcg2 locus in SP cells may be below the threshold required for efficient Cre-mediated recombination. In hematopoietic stem cells, detection of the conditional Rosa26-YFP reporter is low (unpublished data) despite the firmly established expression of Abcg2 in hematopoietic stem cells (Zhou et al., 2001, 2002).

Loss of Abcg2 results in impaired muscle regeneration

In an injury-induced model of muscle regeneration, genetic loss of Abcg2 leads to reduced myogenic proliferation and reduced numbers of myofibers expressing eMyHC. This phenotype is consistent with a loss of total myonuclei, reduced centrally nucleated myofibers, and reduced myofiber size as well as a loss of Pax7+ satellite cells at 30 d after injury. Although the impaired regeneration phenotype in Abcg2$^{-/-}$ mice is not as severe as other models of impaired skeletal muscle regeneration in which both the immune response and angiogenesis are impaired, such as the CCR2-null mice (Contreras-Shannon et al., 2007; Ochoa et al., 2007), it is reminiscent of the resulting impaired muscle regeneration upon partial depletion of monocytes and macrophages (Arnold et al., 2007) or loss of CCL2 (MCP-1; Martinez et al., 2010). Consistent with partial depletion of macrophages, we observe a specific effect on recruitment of antiinflammatory (M2) macrophages. Inhibition of macrophages at day 4 (muscle-loading model) leads to impaired muscle regeneration as measured by central nucleation and impaired satellite cell differentiation (Tidball and Wehling-Henricks, 2007).

In addition, there may be functional compensation from other ABC transporters. Functional compensation by ABC transporters is known to occur; for example, Abcg2 can compensate for loss of mdr1a/1b in hematopoietic stem cells (Zhou et al., 2001). Both mdr1a/1b are expressed in mouse skeletal muscles and could provide compensation for Abcg2 loss in some circumstances (Croop et al., 1989; Israeli et al., 2004).

Impaired skeletal muscle regeneration in Abcg2$^{-/-}$ mice is consistent with a previously identified role for Abcg2 in tissue defense and organ regeneration. In hematopoietic stem cells and cardiac progenitor cells, Abcg2 provides an important cell survival advantage under hypoxic conditions (Krishnamurthy et al., 2004; Martin et al., 2008). Moreover, a recent study demonstrated that Abcg2 has a critical function in cardiac repair after myocardial infarction; specifically, impaired survival of microvascular endothelial cells lead to cardiac rupture in Abcg2$^{-/-}$ mice (Higashikuni et al., 2010). Unlike this myocardial infarction model, the microvasculature appears to be unaffected after injury of skeletal muscle with $BaCl_2$. However, the myocardial infarction model is a more severe injury, and the roles of Abcg2 may be slightly different in the heart and skeletal muscle. Nonetheless, it is likely that Abcg2 provides a critical cell survival function, either through its ability to export genotoxic substrates from the cell or through an unknown novel mechanism in which the ABC transporter affects signaling between cells. This is an attractive hypothesis because cell-autonomous defects in satellite cells from Abcg2$^{-/-}$ mice do not appear to account for the defects observed during regeneration in vivo. Moreover, cells derived from Abcg2-marked cells, including endothelial cells and macrophages, are known to positively regulate myogenesis, and we observe defects in the macrophage response. Additionally, endothelial cells stimulate growth of satellite cells through the secretion of a variety of growth factors, including IGF-1, VEGF, FGF-2, PDGF-BB, and hepatocyte growth factor (Christov et al., 2007). Consistently, we observe modest decreases in angiogenic factors, including HIF1-α, and the angiopoietin genes that could contribute to disrupted signaling during regeneration. The immune response is critical to healthy muscle regeneration, and macrophages have been shown to enhance satellite cell growth and protect satellite cells from apoptosis (Chazaud et al., 2003; Sonnet et al., 2006). The inflammatory response to muscle injury is complex, involving two distinct waves of macrophage infiltration, both proinflammatory and antiinflammatory, that secret cytokines with differing effects on myogenesis and muscle regeneration (Tidball and Villalta, 2010). Interestingly, the proinflammatory cytokines TNF-α and IL-6 are increased, and the chemotactic and activating cytokine CCL-2, which has been previously shown to affect muscle regeneration (Zádor et al., 2001; Warren et al., 2005; Shireman et al., 2007; Martinez et al., 2010), is decreased in Abcg2$^{-/-}$ muscle. The specific effect of loss of *Abcg2* on the antiinflammatory phase of the immune response correlates with the peak in Abcg2

expression at 5 d after injury. Together, these data suggest a role for Abcg2 during muscle regeneration in which it affects signaling between inflammatory and myogenic cells.

Although the mechanism of Abcg2 function remains to be uncovered, here, we demonstrate a physiologically significant function for Abcg2 in regeneration of skeletal muscle. These data highlight the involvement of Abcg2 in a complex biological process involving organ regeneration. Furthermore, these findings contribute to the emerging consensus of muscle healing as a system in which nonmyogenic cells, namely endothelial cells, immune cells, and others, play a critical role in skeletal muscle regeneration.

Materials and methods

Mice

Mice were housed and bred according to National Institutes of Health guidelines for the ethical treatment of animals in a pathogen-free facility. All procedures and protocols were approved by the Institutional Animal Care and Use Committee at the University of Colorado.

$Abcg2^{CreERT2}$ (unpublished data) crossed to the conditional Rosa26-LacZ reporter, Abcg2 knockout mice (Zhou et al., 2002), and mdx^{4cv} (Im et al., 1996) were used. Control mice used were littermate wild-type mice. For injury of the TA muscle, mice were anesthetized, and the right TA muscle was injected with 60 µl of 1.2% $BaCl_2$ (Caldwell et al., 1990) in three places along the muscle. Tamoxifen was prepared at 20 mg/ml in 5% ethanol and sterile maize oil and administered via i.p. injection for a consecutive 3 d at 75 mg per kilogram of mouse weight per day. 10 mg/ml BrdU was injected i.p. 1 h before sacrifice at 50 mg per kilogram of mouse weight.

X-gal staining

Upon harvest, TA muscles were fixed with 4% PFA (in PBS) for 2 h on ice, rinsed with PBS, equilibrated overnight in 30% sucrose, and embedded in optimal cutting temperature freezing medium. Slides with 8-µm sections were processed for X-gal staining. Tissue was postfixed with 0.2% PFA, washed with PBS containing 2 mM $MgCl_2$, and washed with X-gal detergent rinse (0.1 M phosphate buffer, pH 7.3, 2 mM $MgCl_2$, 0.01% Na deoxycholate, and 0.02% IGEPAL CA-630) each for 10 min on ice. Tissue was stained overnight with 1 mg/ml X-gal in detergent rinse containing 20 mM Tris, pH 7.3, 5 mM potassium ferricyanide, and 5 mM potassium ferrocyanide. Sections were counterstained with nuclear fast red and imaged via brightfield microscopy. For X-gal–positive cell scoring, a minimum of three sections were analyzed per biological replica.

Primary cell culture

Satellite cells were obtained as previously described (Pisconti et al., 2010). In brief, hind-limb muscles from 3–6-mo-old mice were harvested, digested with collagenase type I (Worthington) for 1 h at 37°C, filtered, and cultured on gelatin-coated plates in growth medium (F12-C + 15% horse serum + 20 ng/ml FGF-2). For MyHC staining of primary cultures, cells were fixed with AFA (60% EtOH, 3% formaldehyde, and 4% glacial acetic acid). Anti–mouse MyHC (clone MF20; Developmental Studies Hybridoma Bank) was used at 1:10 with anti–mouse biotin-conjugated secondary antibody followed by incubation for 30 min with Vectastain ABC reagent (Vector Laboratories) and developed with DAB (Vector Laboratories). For primary cell scoring, a minimum of 10 fields were scored for Pax7 and MyoD. For fusion index scoring, the total number of myonuclei in MyHC-positive myotubes and the total number of nuclei were counted.

Immunofluorescence

Tissue sections and satellite cells were prepared as previously described from 3–6-mo-old mice (Olguin et al., 2007; Pisconti et al., 2010). For detection of labeled DNA, tissue sections were fixed in methanol for 10 min at −20°C, washed in PBS, permeabilized in PBS + 0.2% Triton X-100 + 1% BSA for 10 min, and denatured in 3 M HCl for 20 min before incubation with primary antibodies overnight at 4°C in PBS + 10% horse serum. Primary antibodies used for immunofluorescence were chicken polyclonal β-galactosidase (Immunology Consultants Laboratory, Inc.) at 1:500, rabbit polyclonal anti-NG2 (Millipore) at 1:200, rat anti-CD31 (BD) at 1:200, rat anti–Sca-1 (BD) at 1:200, rat polyclonal anti-BrdU (AbD Serotec) at 1:100, rabbit polyclonal antilaminin (Sigma-Aldrich) at 1:200, rat anti-F4/80 (Genetex) at 1:500, mouse anti-Pax7 (Developmental Studies Hybridoma Bank) at 1:100, rabbit anti-MyoD (Santa Cruz Biotechnology, Inc.) at 1:800, and mouse monoclonal eMyHC (Developmental Studies Hybridoma Bank), neat. For eMyHC and Pax7 staining, a fluorescein immunodetection kit (Mouse on Mouse; Vector Laboratories) was used per the manufacturer's directions. Secondary antibodies conjugated with Alexa Fluor 488, Alexa Fluor 555, or Alexa Fluor 594 (Invitrogen) were used at a 1:1,000 dilution. Vectashield with DAPI (Vector Laboratories) was used as mounting media.

Morphometric analysis

Myofiber cross-sectional area, number of myonuclei, and number of BrdU-positive cells in injured TA muscle were quantified via manual masking using SlideBook (Intelligent Imaging Innovations) based on dystrophin or BrdU and DAPI staining in 40× fields. The number of satellite cells was quantified based on Pax7 staining and sublaminar localization. A minimum of 500 myofibers and three sections were analyzed per biological replica.

Flow cytometry

Primary muscle cells were isolated from adult mouse hind-limb muscles or TA muscles as previously described (Tanaka et al., 2009). In brief, isolated muscle was digested with type I collagenase (Worthington) for 1 h at 37°C, filtered, and recovered in F12-C with 15% horse serum and 0.5 nM FGF-2. For antibody labeling, cells were incubated for 45 min at 4°C with mouse Abcg2 (Bcrp1, clone 5D3; BD) at 1:100 followed by anti–mouse IgG–PE-Cy5 (Santa Cruz Biotechnology, Inc.) secondary antibody. For FDG (Invitrogen) labeling, an equal volume of cells and 2 mM FDG were mixed and incubated at 37°C for 1 min. 10 vol cold media was added, and cells were recovered on ice for 1 h. Cells were then incubated with the following antibodies at 4°C for 30 min: rat anti–Sca-1–PE conjugated (BD) at 1:200, rat anti-CD31–PE conjugated (BD) at 1:200, rat anti-CD45–PeCy7 conjugated (BD) at 1:400, rat anti–α7-integrin–Alexa Fluor 647 conjugated (AbLab, University of British Columbia) at 1:1,000, rat anti-CD34–Alexa Fluor 647 (BD) conjugated at 1:100, and rat anti-PDGF-R-α–allophycocyanin conjugated (eBioscience) at 1:200. DAPI was added at 1 µg/ml to exclude dead cells. Cell analysis was performed with an ADP three-laser flow cytometer (CyAn; Beckman Coulter). Appropriate fluorescence minus one controls were used to set gates to <1% background. Data were analyzed after sort with FlowJo software (Tree Star).

RNA isolation and quantitative RT-PCR

TA muscles 3 d after $BaCl_2$-induced injury and uninjured contralateral control from wild-type and $Abcg2^{-/-}$ mice were harvested and homogenized, and RNA was isolated using a purification kit (RNAqueous; Invitrogen). cDNA was made using reverse transcriptase (Superscript III; Invitrogen) with random hexamer primers, and quantitative PCR was performed using SYBR green (Applied Biosystems) and gene specific primers as previously published (Higashikuni et al., 2010).

Microscopy, image processing, and figure preparation

Brightfield images were acquired with a microscope (DM5500; Leica) using Metamorph software (Molecular Devices) coupled with a camera (DFC; Leica). Objectives used were HC Plan Apochromat 20×/NA 0.70 or HCX Plan Apochromat 40× oil/NA 1.25–0.75 (Leica). Fluorescent micrographs were taken with a confocal microscope (LSM 5; Carl Zeiss) using ZEN 2009 software (Carl Zeiss) or with an epifluorescence microscope (Eclipse E800; Nikon) using SlideBook v4.1 acquisition software coupled to a digital camera (Sensicam; Cooke). Lenses used with the confocal microscope were Plan Apochromat 63× oil/NA 1.4 differential interference contrast M27 (Carl Zeiss). Lenses used with the epifluorescence microscope were Plan Fluor either 40×/NA 0.75 differential interference contrast M or 20×/NA 0.50 Ph1 DLL (Nikon). All digital microscopic images were acquired at room temperature. Mounting medium (Vectashield) was used for imaging. The fluorochromes used were Alexa Fluor 488 and Alexa Fluor 594 or Alexa Fluor 555 (confocal) conjugated to secondary antibodies for immunofluorescence as indicated in the Immunofluorescence section. For figure preparation, images were exported in Photoshop (Adobe), if necessary, brightness and contrast were adjusted for the entire image, the image was cropped, and individual color channels were extracted (when required) without color correction or γ adjustments.

Statistical analysis

All data are presented as means ± SEM. Student's *t* test (unpaired and two tailed) was used to determine the statistical significance of individual datasets in Prism (version 5; GraphPad Software). Differences are considered significant for $P < 0.05$, very significant for $P < 0.01$, and highly significant for $P < 0.001$.

Online supplemental material

Fig. S1 shows that *Abcg2*$^{-/-}$ satellite cells differentiate normally when isolated and cultured and is related to Table I. Fig. S2 shows punctate staining of X-gal in muscle sections isolated from tamoxifen-treated *Actin*^{CreERT2}*;R26R* and *Abcg2*^{CreERT2}*;R26R* and is related to Fig. 5. Online supplemental material is available at http://www.jcb.org/cgi/content/full/jcb.201103159/DC1.

We thank Kelly Dunn and Nicole Dalla Betta for technical assistance and members of the Olwin laboratory for critical reading of the manuscript. The Pax7, MF20, and eMyHC monoclonal antibodies were obtained from the Developmental Studies Hybridoma Bank developed under the auspices of the National Institute of Child Health and Human Development and maintained by The University of Iowa Department of Biology.

The project described was supported by National Institutes of Health grants F32-AR056565 to M.J. Doyle and AR039467 and AR04496 to B.B. Olwin and a grant from the Muscular Dystrophy Association to B.B. Olwin.

Submitted: 29 March 2011
Accepted: 31 August 2011

References

Abou-Khalil, R., R. Mounier, and B. Chazaud. 2010. Regulation of myogenic stem cell behavior by vessel cells: the "ménage à trois" of satellite cells, periendothelial cells and endothelial cells. *Cell Cycle*. 9:892–896. http://dx.doi.org/10.4161/cc.9.5.10851

Arnold, L., A. Henry, F. Poron, Y. Baba-Amer, N. van Rooijen, A. Plonquet, R.K. Gherardi, and B. Chazaud. 2007. Inflammatory monocytes recruited after skeletal muscle injury switch into antiinflammatory macrophages to support myogenesis. *J. Exp. Med.* 204:1057–1069. http://dx.doi.org/10.1084/jem.20070075

Asakura, A., P. Seale, A. Girgis-Gabardo, and M.A. Rudnicki. 2002. Myogenic specification of side population cells in skeletal muscle. *J. Cell Biol.* 159:123–134. http://dx.doi.org/10.1083/jcb.200202092

Beauchamp, J.R., L. Heslop, D.S. Yu, S. Tajbakhsh, R.G. Kelly, A. Wernig, M.E. Buckingham, T.A. Partridge, and P.S. Zammit. 2000. Expression of CD34 and Myf5 defines the majority of quiescent adult skeletal muscle satellite cells. *J. Cell Biol.* 151:1221–1234. http://dx.doi.org/10.1083/jcb.151.6.1221

Blanco-Bose, W.E., C.C. Yao, R.H. Kramer, and H.M. Blau. 2001. Purification of mouse primary myoblasts based on alpha 7 integrin expression. *Exp. Cell Res.* 265:212–220. http://dx.doi.org/10.1006/excr.2001.5191

Caldwell, C.J., D.L. Mattey, and R.O. Weller. 1990. Role of the basement membrane in the regeneration of skeletal muscle. *Neuropathol. Appl. Neurobiol.* 16:225–238. http://dx.doi.org/10.1111/j.1365-2990.1990.tb01159.x

Chazaud, B., C. Sonnet, P. Lafuste, G. Bassez, A.C. Rimaniol, F. Poron, F.J. Authier, P.A. Dreyfus, and R.K. Gherardi. 2003. Satellite cells attract monocytes and use macrophages as a support to escape apoptosis and enhance muscle growth. *J. Cell Biol.* 163:1133–1143. http://dx.doi.org/10.1083/jcb.200212046

Christov, C., F. Chrétien, R. Abou-Khalil, G. Bassez, G. Vallet, F.J. Authier, Y. Bassaglia, V. Shinin, S. Tajbakhsh, B. Chazaud, and R.K. Gherardi. 2007. Muscle satellite cells and endothelial cells: close neighbors and privileged partners. *Mol. Biol. Cell*. 18:1397–1409. http://dx.doi.org/10.1091/mbc.E06-08-0693

Contreras-Shannon, V., O. Ochoa, S.M. Reyes-Reyna, D. Sun, J.E. Michalek, W.A. Kuziel, L.M. McManus, and P.K. Shireman. 2007. Fat accumulation with altered inflammation and regeneration in skeletal muscle of CCR2−/− mice following ischemic injury. *Am. J. Physiol. Cell Physiol.* 292:C953–C967. http://dx.doi.org/10.1152/ajpcell.00154.2006

Croop, J.M., M. Raymond, D. Haber, A. Devault, R.J. Arceci, P. Gros, and D.E. Housman. 1989. The three mouse multidrug resistance (mdr) genes are expressed in a tissue-specific manner in normal mouse tissues. *Mol. Cell. Biol.* 9:1346–1350.

Dellavalle, A., M. Sampaolesi, R. Tonlorenzi, E. Tagliafico, B. Sacchetti, L. Perani, A. Innocenzi, B.G. Galvez, G. Messina, R. Morosetti, et al. 2007. Pericytes of human skeletal muscle are myogenic precursors distinct from satellite cells. *Nat. Cell Biol.* 9:255–267. http://dx.doi.org/10.1038/ncb1542

Ferrari, G., G. Cusella-De Angelis, M. Coletta, E. Paolucci, A. Stornaiuolo, G. Cossu, and F. Mavilio. 1998. Muscle regeneration by bone marrow-derived myogenic progenitors. *Science*. 279:1528–1530. http://dx.doi.org/10.1126/science.279.5356.1528

Gussoni, E., Y. Soneoka, C.D. Strickland, E.A. Buzney, M.K. Khan, A.F. Flint, L.M. Kunkel, and R.C. Mulligan. 1999. Dystrophin expression in the mdx mouse restored by stem cell transplantation. *Nature*. 401:390–394.

Higashikuni, Y., J. Sainz, K. Nakamura, M. Takaoka, S. Enomoto, H. Iwata, M. Sahara, K. Tanaka, N. Koibuchi, S. Ito, et al. 2010. The ATP-binding cassette transporter BCRP1/ABCG2 plays a pivotal role in cardiac repair after myocardial infarction via modulation of microvascular endothelial cell survival and function. *Arterioscler. Thromb. Vasc. Biol.* 30:2128–2135. http://dx.doi.org/10.1161/ATVBAHA.110.211755

Huls, M., F.G. Russel, and R. Masereeuw. 2009. The role of ATP binding cassette transporters in tissue defense and organ regeneration. *J. Pharmacol. Exp. Ther.* 328:3–9. http://dx.doi.org/10.1124/jpet.107.132225

Im, W.B., S.F. Phelps, E.H. Copen, E.G. Adams, J.L. Slightom, and J.S. Chamberlain. 1996. Differential expression of dystrophin isoforms in strains of mdx mice with different mutations. *Hum. Mol. Genet.* 5:1149–1153. http://dx.doi.org/10.1093/hmg/5.8.1149

Israeli, D., R. Benchaouir, S. Ziaei, P. Rameau, C. Gruszczynski, E. Peltekian, O. Danos, and L. Garcia. 2004. FGF6 mediated expansion of a resident subset of cells with SP phenotype in the C2C12 myogenic line. *J. Cell. Physiol.* 201:409–419. http://dx.doi.org/10.1002/jcp.20088

Joe, A.W., L. Yi, A. Natarajan, F. Le Grand, L. So, J. Wang, M.A. Rudnicki, and F.M. Rossi. 2010. Muscle injury activates resident fibro/adipogenic progenitors that facilitate myogenesis. *Nat. Cell Biol.* 12:153–163. http://dx.doi.org/10.1038/ncb2015

Krishnamurthy, P., and J.D. Schuetz. 2006. Role of ABCG2/BCRP in biology and medicine. *Annu. Rev. Pharmacol. Toxicol.* 46:381–410. http://dx.doi.org/10.1146/annurev.pharmtox.46.120604.141238

Krishnamurthy, P., D.D. Ross, T. Nakanishi, K. Bailey-Dell, S. Zhou, K.E. Mercer, B. Sarkadi, B.P. Sorrentino, and J.D. Schuetz. 2004. The stem cell marker Bcrp/ABCG2 enhances hypoxic cell survival through interactions with heme. *J. Biol. Chem.* 279:24218–24225. http://dx.doi.org/10.1074/jbc.M313599200

Luth, E.S., S.J. Jun, M.K. Wessen, K. Liadaki, E. Gussoni, and L.M. Kunkel. 2008. Bone marrow side population cells are enriched for progenitors capable of myogenic differentiation. *J. Cell Sci.* 121:1426–1434. http://dx.doi.org/10.1242/jcs.021675

Martin, C.M., A.P. Meeson, S.M. Robertson, T.J. Hawke, J.A. Richardson, S. Bates, S.C. Goetsch, T.D. Gallardo, and D.J. Garry. 2004. Persistent expression of the ATP-binding cassette transporter, Abcg2, identifies cardiac SP cells in the developing and adult heart. *Dev. Biol.* 265:262–275. http://dx.doi.org/10.1016/j.ydbio.2003.09.028

Martin, C.M., A. Ferdous, T. Gallardo, C. Humphries, H. Sadek, A. Caprioli, J.A. Garcia, L.I. Szweda, M.G. Garry, and D.J. Garry. 2008. Hypoxia-inducible factor-2alpha transactivates Abcg2 and promotes cytoprotection in cardiac side population cells. *Circ. Res.* 102:1075–1081. http://dx.doi.org/10.1161/CIRCRESAHA.107.161729

Martinez, C.O., M.J. McHale, J.T. Wells, O. Ochoa, J.E. Michalek, L.M. McManus, and P.K. Shireman. 2010. Regulation of skeletal muscle regeneration by CCR2-activating chemokines is directly related to macrophage recruitment. *Am. J. Physiol. Regul. Integr. Comp. Physiol.* 299:R832–R842. http://dx.doi.org/10.1152/ajpregu.00797.2009

Meeson, A.P., T.J. Hawke, S. Graham, N. Jiang, J. Elterman, K. Hutcheson, J.M. Dimaio, T.D. Gallardo, and D.J. Garry. 2004. Cellular and molecular regulation of skeletal muscle side population cells. *Stem Cells*. 22:1305–1320. http://dx.doi.org/10.1634/stemcells.2004-0077

Mitchell, K.J., A. Pannérec, B. Cadot, A. Parlakian, V. Besson, E.R. Gomes, G. Marazzi, and D.A. Sassoon. 2010. Identification and characterization of a non-satellite cell muscle resident progenitor during postnatal development. *Nat. Cell Biol.* 12:257–266.

Mitchell, P.O., T. Mills, R.S. O'Connor, E.R. Kline, T. Graubert, E. Dzierzak, and G.K. Pavlath. 2005. Sca-1 negatively regulates proliferation and differentiation of muscle cells. *Dev. Biol.* 283:240–252. http://dx.doi.org/10.1016/j.ydbio.2005.04.016

Montarras, D., J. Morgan, C. Collins, F. Relaix, S. Zaffran, A. Cumano, T. Partridge, and M. Buckingham. 2005. Direct isolation of satellite cells for skeletal muscle regeneration. *Science*. 309:2064–2067. http://dx.doi.org/10.1126/science.1114758

Ochoa, O., D. Sun, S.M. Reyes-Reyna, L.L. Waite, J.E. Michalek, L.M. McManus, and P.K. Shireman. 2007. Delayed angiogenesis and VEGF production in CCR2−/− mice during impaired skeletal muscle regeneration. *Am. J. Physiol. Regul. Integr. Comp. Physiol.* 293:R651–R661. http://dx.doi.org/10.1152/ajpregu.00069.2007

Ojima, K., A. Uezumi, H. Miyoshi, S. Masuda, Y. Morita, A. Fukase, A. Hattori, H. Nakauchi, Y. Miyagoe-Suzuki, and S. Takeda. 2004. Mac-1(low) early myeloid cells in the bone marrow-derived SP fraction migrate into injured skeletal muscle and participate in muscle regeneration. *Biochem. Biophys. Res. Commun.* 321:1050–1061. http://dx.doi.org/10.1016/j.bbrc.2004.07.069

Olguin, H.C., Z. Yang, S.J. Tapscott, and B.B. Olwin. 2007. Reciprocal inhibition between Pax7 and muscle regulatory factors modulates myogenic cell fate determination. *J. Cell Biol.* 177:769–779. http://dx.doi.org/10.1083/jcb.200608122

Péault, B., M. Rudnicki, Y. Torrente, G. Cossu, J.P. Tremblay, T. Partridge, E. Gussoni, L.M. Kunkel, and J. Huard. 2007. Stem and progenitor cells in skeletal muscle development, maintenance, and therapy. *Mol. Ther.* 15:867–877. http://dx.doi.org/10.1038/mt.sj.6300145

Pisconti, A., D.D. Cornelison, H.C. Olguín, T.L. Antwine, and B.B. Olwin. 2010. Syndecan-3 and Notch cooperate in regulating adult myogenesis. *J. Cell Biol.* 190:427–441. http://dx.doi.org/10.1083/jcb.201003081

Polesskaya, A., P. Seale, and M.A. Rudnicki. 2003. Wnt signaling induces the myogenic specification of resident CD45+ adult stem cells during muscle regeneration. *Cell*. 113:841–852. http://dx.doi.org/10.1016/S0092-8674(03)00437-9

Rivier, F., O. Alkan, A.F. Flint, K. Muskiewicz, P.D. Allen, P. Leboulch, and E. Gussoni. 2004. Role of bone marrow cell trafficking in replenishing skeletal muscle SP and MP cell populations. *J. Cell Sci.* 117:1979–1988. http://dx.doi.org/10.1242/jcs.01051

Sacco, A., R. Doyonnas, P. Kraft, S. Vitorovic, and H.M. Blau. 2008. Self-renewal and expansion of single transplanted muscle stem cells. *Nature*. 456:502–506. http://dx.doi.org/10.1038/nature07384

Shireman, P.K., V. Contreras-Shannon, O. Ochoa, B.P. Karia, J.E. Michalek, and L.M. McManus. 2007. MCP-1 deficiency causes altered inflammation with impaired skeletal muscle regeneration. *J. Leukoc. Biol.* 81:775–785. http://dx.doi.org/10.1189/jlb.0506356

Sonnet, C., P. Lafuste, L. Arnold, M. Brigitte, F. Poron, F.J. Authier, F. Chrétien, R.K. Gherardi, and B. Chazaud. 2006. Human macrophages rescue myoblasts and myotubes from apoptosis through a set of adhesion molecular systems. *J. Cell Sci.* 119:2497–2507. http://dx.doi.org/10.1242/jcs.02988

Soriano, P. 1999. Generalized lacZ expression with the ROSA26 Cre reporter strain. *Nat. Genet.* 21:70–71. http://dx.doi.org/10.1038/5007

Tamaki, T., A. Akatsuka, K. Ando, Y. Nakamura, H. Matsuzawa, T. Hotta, R.R. Roy, and V.R. Edgerton. 2002. Identification of myogenic-endothelial progenitor cells in the interstitial spaces of skeletal muscle. *J. Cell Biol.* 157:571–577. http://dx.doi.org/10.1083/jcb.200112106

Tanaka, K.K., J.K. Hall, A.A. Troy, D.D. Cornelison, S.M. Majka, and B.B. Olwin. 2009. Syndecan-4-expressing muscle progenitor cells in the SP engraft as satellite cells during muscle regeneration. *Cell Stem Cell*. 4:217–225. http://dx.doi.org/10.1016/j.stem.2009.01.016

Tidball, J.G., and S.A. Villalta. 2010. Regulatory interactions between muscle and the immune system during muscle regeneration. *Am. J. Physiol. Regul. Integr. Comp. Physiol.* 298:R1173–R1187. http://dx.doi.org/10.1152/ajpregu.00735.2009

Tidball, J.G., and M. Wehling-Henricks. 2007. Macrophages promote muscle membrane repair and muscle fibre growth and regeneration during modified muscle loading in mice in vivo. *J. Physiol.* 578:327–336. http://dx.doi.org/10.1113/jphysiol.2006.118265

Uezumi, A., S. Fukada, N. Yamamoto, S. Takeda, and K. Tsuchida. 2010. Mesenchymal progenitors distinct from satellite cells contribute to ectopic fat cell formation in skeletal muscle. *Nat. Cell Biol.* 12:143–152. http://dx.doi.org/10.1038/ncb2014

Warren, G.L., T. Hulderman, N. Jensen, M. McKinstry, M. Mishra, M.I. Luster, and P.P. Simeonova. 2002. Physiological role of tumor necrosis factor alpha in traumatic muscle injury. *FASEB J.* 16:1630–1632.

Warren, G.L., T. Hulderman, D. Mishra, X. Gao, L. Millecchia, L. O'Farrell, W.A. Kuziel, and P.P. Simeonova. 2005. Chemokine receptor CCR2 involvement in skeletal muscle regeneration. *FASEB J.* 19:413–415.

Zádor, E., L. Mendler, V. Takács, J. de Bleecker, and F. Wuytack. 2001. Regenerating soleus and extensor digitorum longus muscles of the rat show elevated levels of TNF-alpha and its receptors, TNFR-60 and TNFR-80. *Muscle Nerve*. 24:1058–1067. http://dx.doi.org/10.1002/mus.1110

Zheng, B., B. Cao, M. Crisan, B. Sun, G. Li, A. Logar, S. Yap, J.B. Pollett, L. Drowley, T. Cassino, et al. 2007. Prospective identification of myogenic endothelial cells in human skeletal muscle. *Nat. Biotechnol.* 25:1025–1034. http://dx.doi.org/10.1038/nbt1334

Zhou, S., J.D. Schuetz, K.D. Bunting, A.M. Colapietro, J. Sampath, J.J. Morris, I. Lagutina, G.C. Grosveld, M. Osawa, H. Nakauchi, and B.P. Sorrentino. 2001. The ABC transporter Bcrp1/ABCG2 is expressed in a wide variety of stem cells and is a molecular determinant of the side-population phenotype. *Nat. Med.* 7:1028–1034. http://dx.doi.org/10.1038/nm0901-1028

Zhou, S., J.J. Morris, Y. Barnes, L. Lan, J.D. Schuetz, and B.P. Sorrentino. 2002. Bcrp1 gene expression is required for normal numbers of side population stem cells in mice, and confers relative protection to mitoxantrone in hematopoietic cells in vivo. *Proc. Natl. Acad. Sci. USA*. 99:12339–12344. http://dx.doi.org/10.1073/pnas.192276999